Pergamon

Quaternary Science Reviews, Vol. 17, pp. 43–75, 1998

0277-3791/98 $19.00

PII: S0277–3791(97)00066-8

THE LAST GLACIAL MAXIMUM OF SVALBARD AND THE BARENTS SEA AREA: ICE SHEET EXTENT AND CONFIGURATION

JON Y. LANDVIK†, STEIN BONDEVIK‡, ANDERS ELVERHØI§, WILLY FJELDSKAAR¶, JAN MANGERUD‡, OTTO SALVIGSEN‡‡, MARTIN J. SIEGERT††, JOHN-INGE SVENDSEN§§, TORE O. VORREN¶¶

† *The University Courses on Svalbard (UNIS), P.O. Box 156, N-9170 Longyearbyen, Norway (E-mail: jan.Landvik@unis.no)*

‡ *University of Bergen, Department of Geology, Allégt. 41, N-5007 Bergen, Norway*

§ *University of Oslo, Department of Geology, P.O. Box 1047 Blindern, N-0316 Oslo, Norway*

¶ *Rogaland Research, P.O. Box 2503, N-4004 Stavanger, Norway*

†† *University of Wales, Centre for Glaciology, Institute of Earth Studies, Aberystwyth, Dyfed SY23 3DB Wales, UK*

‡‡ *Norwegian Polar Institute, P.O. Box 5072, Majorstua, N-0301 Oslo, Norway*

§§ *University of Bergen, Centre for Studies of Environment and Resources, N-5020 Bergen, Norway*

¶¶ *University of Tromsø, Department of Geology, N-9037 Tromsø, Norway*

Abstract—The timing, extent and configuration of the Late Weichselian Barents ice sheet has been debated for several decades. This debate has arisen largely because of the limited or conflicting field evidence on which most models have been based. In particular, reconstruction of the marine parts of the former Barents ice sheet has been controversial. This paper aims to review the geological observations and interpretations regarding the size and timing of the Late Weichselian ice sheet, combined with numerical modelling of its formation in order to produce a reconstruction of ice sheet extent and behaviour. Sub-glacial till with overlying glacimarine deposits dated to the Late Weichselian is found over most of the Barents Sea floor and the continental shelf west of Svalbard. Glacially induced debris flow deposits on the large Bjørnøya and Isfjorden trough mouth fans strongly support the idea of ice sheet extension to the shelf edge during maximum glaciation. Isobase maps show a centre of post-glacial uplift in the north-central Barents Sea, and glaciological and isostatic modelling suggest that the ice sheet was 2000–3000 m thick in this area. The ice sheet was confluent with ice over the Kara Sea, but the interaction between the Barents and Kara ice sheets is not yet fully understood. The deglaciation of the Barents ice sheet started ca 15 ka, probably by calving within the deeper troughs. By 12 ka, most of the central Barents Sea was ice free, and ice remained over the Svalbard, Franz Josef Land and Novaja Zemlya archipelagos and adjacent shallow shelf areas. The coasts and fjords of these islands were ice free by 10 ka.

INTRODUCTION

For the last three decades, the extent of the Late Weichselian ice sheet over Svalbard and the Barents Sea (Fig. 1) has been subject to one of the most fascinating scientific discussions regarding the glacial history of the Arctic. Although scientists have agreed on the location of ice margins around many of the former northern hemisphere ice sheets, the suggested reconstructions for the Svalbard–Barents Sea region range from almost no glacier ice to complete grounded ice cover of the region. At the last glacial maximum, this marine-based Barents Sea ice sheet played an important role in the climatic history of the region through interaction with the oceans bordering the ice sheet to the west and the north.

A large marine-based ice sheet in the Barents Sea during the last glaciation was first proposed by de Geer (1900). His model of a glaciated Barents Sea was generally accepted for a number of decades, until renewed field studies in the 1960s and 1970s failed to prove such an extensive glaciation (Lavrushin, 1969; Boulton, 1979a,b; Troitsky *et al.*, 1979; Matishov, 1980). However, the conclusions from these studies were in contrast to those of Andersen (1981) and Denton *et al.* (1981), who, based on a thorough review of geological data, suggested an almost total ice-sheet cover of Svalbard and the Barents shelf as the most likely Late Weichselian scenario. An important argument relating to the glacial extent was the pattern of Holocene glacioisostatic rebound. This had been mapped by Schytt

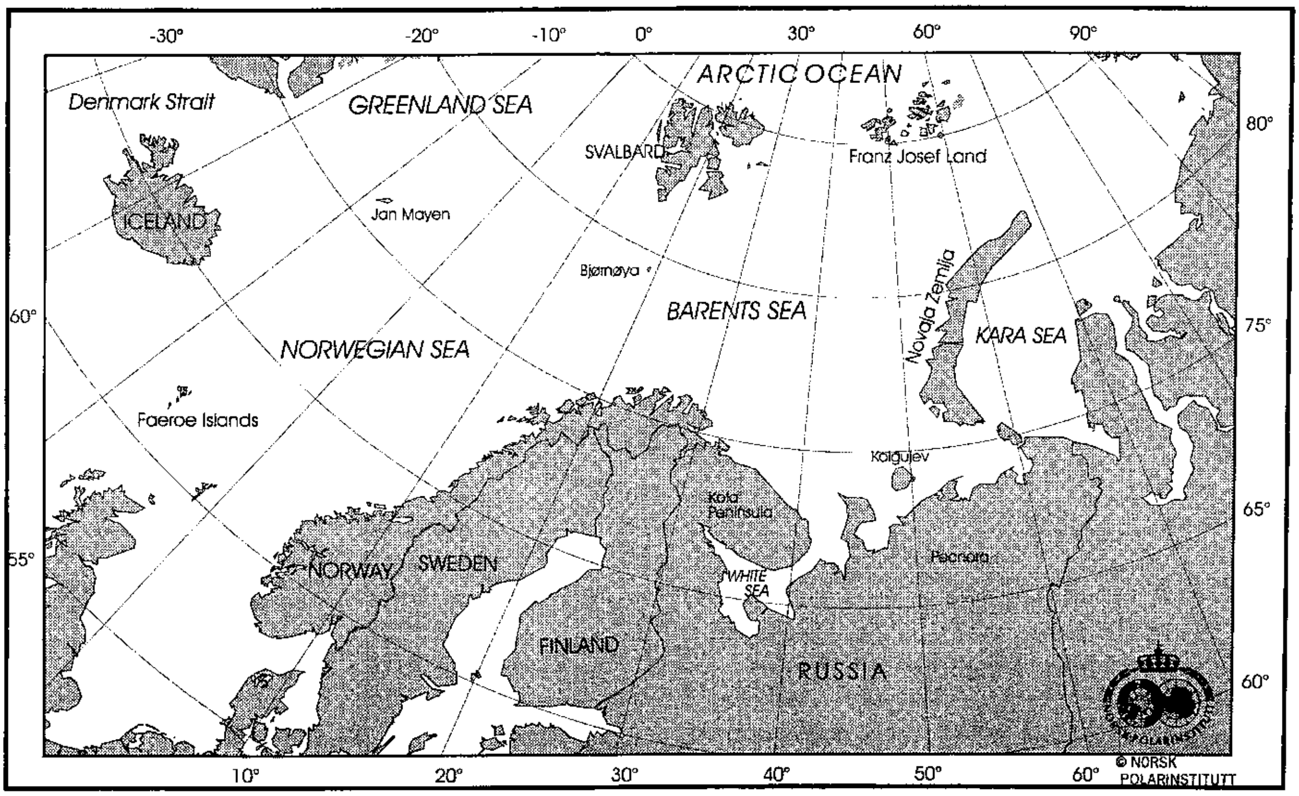

FIG. 1. The Barents Sea, bordering ocean and land masses.

et al. (1968) and suggested that at 6.5 ka there was a centre of postglacial uplift in the northern Barents Sea. The question of extensive glaciation of Svalbard and the northern Barents Sea was resolved when driftwood dated to almost 10 ka was found at 100 m elevation on Kongsoya Land (Salvigsen, 1981), requiring that a large ice load had existed over the region some time during the Late Weichselian. Based on detailed terrestrial and marine field studies, Mangerud *et al.* (1992) demonstrated that the Late Weichselian ice margin reached beyond the coastline of western Svalbard. Marine geological studies in both the Barents Sea (e.g. Elverhøi and Solheim, 1983a,b; Vorren and Kristoffersen, 1986; Solheim *et al.*, 1990; Elverhøi *et al.*, 1993) and on the Svalbard shelf (Mangerud *et al.*, 1992; Svendsen *et al.*, 1992) during the 1980s have also contributed to the documentation of an extensive glaciation model through mapping and age estimates of glacial tills and sub-glacial flutes (Fig. 2).

Extensive investigations in the Svalbard and Barents Sea region have resulted in a significant increase in geological data since the last extensive review by Andersen (1981). In this paper, we review the present data that allow a new and improved reconstruction of the Late Weichselian ice limits. These include a wide range of observations, including sediment sections on land, offshore sediment cores and seismic profiles, relative sea-level changes and geomorphology. The ice-sheet reconstruction obtained from the geological observations is compared with results from numerical glaciological and isostatic modelling to obtain quantitative information concerning the geometry of the ice sheet, and the processes that controlled its growth and decay.

In a glaciated region, the completeness of the stratigraphic record and, thus, the resolution of the reconstructed history, decreases drastically with each successive glaciation. In this chapter we discuss the Late Weichselian glaciation in greater detail than is possible for earlier glaciations. However, this conceptual glaciation model can be used to understand earlier glaciations throughout the last interglacial-glacial cycle (see Mangerud *et al.*, 1998).

GEOLOGICAL OBSERVATIONS

Svalbard and the western shelf

In the Svalbard region (Fig. 1), the debate whether a limited or a large ice sheet existed during the Late Weichselian originated from studies on the main island of Spitsbergen (Fig. 2). Based on investigations of the stratigraphy at Kapp Ekholm in Billefjorden, and other sections, Lavrushin (1969), Boulton (1979a) and Troitsky *et al.* (1979) suggested that the glaciers only advanced slightly beyond their present margins during the Late Weichselian. However, the same authors disagreed on the timing of this advance. Troitsky *et al.* (1979) also proposed that the advance occurred as

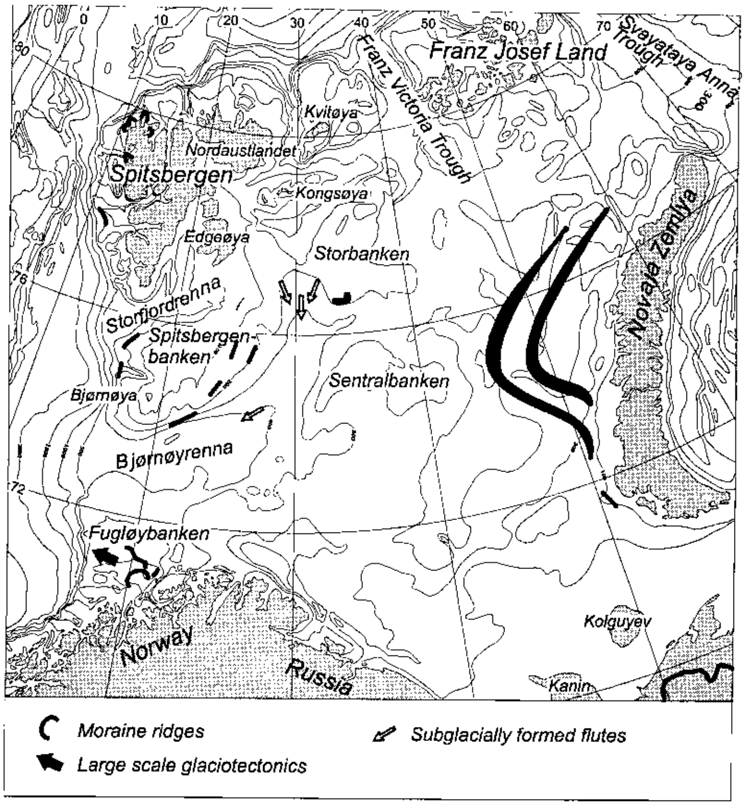

FIG. 2. Selected large-scale geomorphic features related to the Late Weichselian ice sheet in the Svalbard–Barents Sea area. Contour interval 100 m.

early as 26 ka on the basis of a thermoluminescence age estimate from glacial sediments south of Bellsund, whereas Boulton (1979a) assigned a Younger Dryas age (the Billefjorden event on the basis of his investigations at Kapp Ekholm. Reports of glacially undisturbed raised beaches older than the Late Weichselian from the coast between Kongsfjorden and Isfjorden (Fig. 4) supported the assumption that the area had been ice free since at least since the Middle Weichselian (Salvigsen, 1977; Boulton *et al.*, 1982; Miller, 1982; Forman and Miller, 1984; Forman, 1989; Lehman and Forman, 1992).

A key question is whether a lack of till or other sub-glacially formed features overlying these pre-Late Weichselian beaches really proves that the sites were not overrun by glacier ice. The opposite is demonstrated in KongsfJorden, where apparently undisturbed Middle Weichselian beach sediments were found on the proximal side of a terminal moraine dated to ca 13 ka (Lehman and Forman, 1992). From the south shore of Isfjorden, Mangerud *et al.* (1992) showed that even the morphology of a beach terrace dated to 36 ka was preserved after the glacier overrode the terrace. These two case studies demonstrate that it is difficult to prove non-glaciation based on non-deposition. We, therefore, consider it important to base our reconstruction in this paper on stratigraphic and geomorphic evidence of glaciation (Fig. 2) and associated radiocarbon ages (Fig. 3).

Although if the present geological reconstruction shows that Late Weichselian ice covered both Svalbard and the Barents Sea, this ice sheet most likely resulted from the interplay between several separate ice domes and accumulation areas (Landvik and Salvigsen, 1985; Forman, 1989; Mangerud *et al.*, 1992). In particular, the high relief, valleys and fjords of the Svalbard archipelago must have had a substantial influence on the ice flow. Due to these regional differences in ice accumulation and drainage, we discuss separately the extent of the last ice advance within the different fjord systems and the adjacent parts of the continental shelf off Svalbard.

Northwest Spitsbergen

The northwest corner of Spitsbergen from Woodfjorden to Kongsfjorden (Fig. 4) is characterised by the large Reinsdyrflya strandflat to the east, and a more alpine topography with a relief up to 1000 m a.s.l. to the west. The continental shelf extends for 80–100 km to the north and west of the coast. The northwesternmost islands, Danskøya and Amsterdamøya, lie almost at the shelf break (Figs. 3 and 4). In contrast to the rest of Svalbard, the geological record on land in this area shows well-preserved pre-Holocene glacial features such as terminal moraines, glacial striae and meltwater channels (Salvigsen, 1977; Salvigsen and Österholm, 1982).

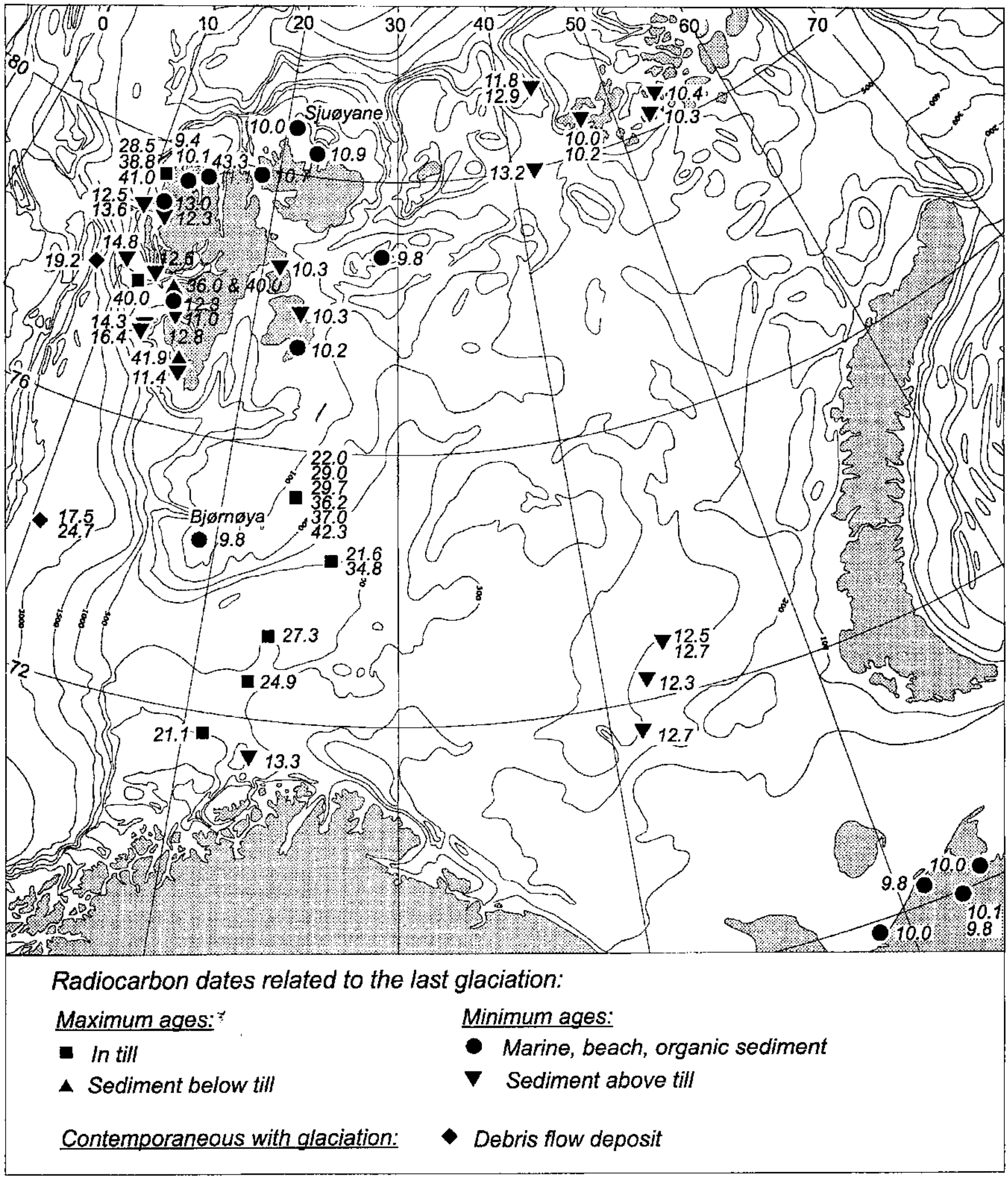

FIG. 3. Key radiocarbon age estimates used to delimit the Late Weichselian ice sheet. The ages represent a selection focused on highlighting the last glacial advance. For some sites two or more corresponding ages are shown. Details of the radiocarbon ages can be found in Table 1. Place names are given in Fig. 2.

In Woodfjorden and Liefdefjorden, a minimum extent of the Late Weichselian ice sheet is marked by the terminal moraines and lateral melt-water channels near the mouth of Liefdefjorden (Figs. 2 and 4) (Salvigsen and Österholm, 1982). The marine limit on the proximal side of the moraines is 23 m a.s.l. on Reinsdyrflya, distal to the moraines, undisturbed beaches as high as 90 m a.s.l. have radiocarbon ages of > 40 ka (Salvigsen and Österholm, 1982). They postulated that retreat from the moraines occurred prior to 11–10.5 ka based on correlation of shore lines along the fjord. Glacial striae and erratics indicate that a local Late

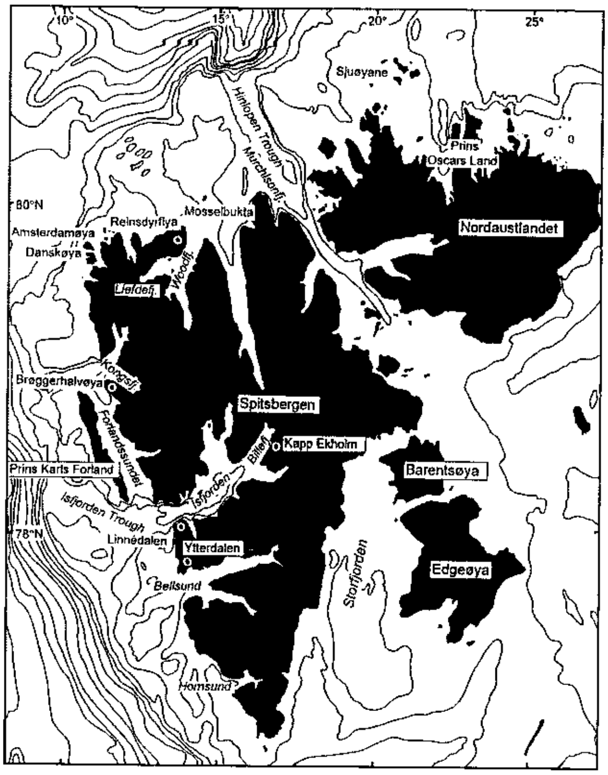

FIG. 4. Detail map of the west coast of Svalbard and the adjacent shelf with place names used in the text. Contour interval is 100, 200, 400, 600 m, etc.

Weichselian ice cap was centred west of Liefdefjorden (Salvigsen and Österholm, 1982). The ice-marginal features in Liefdefjorden were assumed to have formed along the eastern limit of this ice sheet and, thus, be synchronous with the submarine moraines discovered by Liestøl (1972) (see below). A sea-eroded section in the morainic ridge in Liefdefjorden shows sublittoral sand underlying till and containing calcareous algae (*Lithothamnion* sp.) dated at 34 ka (Table 1). However, unpublished data by A. Solheim (*pers. comm.*, 1996) on the fjord sediments show that there is no change in sediment thickness across the reconstructed ice margin position as one would expect if the maximum limit for the Late Weichselian glacier had been located here. We find it likely that these marginal features record a retreat stage in Liefdefjorden, and that the Late Weichselian glacier extended further out, removing older sediments from the Liefdefjorden and Woodfjorden basins.

On the inner shelf off Raudfjorden, Smeerenburgfjorden and in the sound between Amsterdamøya and Danskøya (Fig. 5), well-developed submarine moraines were deposited in front of glaciers that filled the fjords (Liestøl, 1972). Proximal to the moraines are several sites on land where marine sediments have been incorporated into tills or have been glacially dislocated. Shells in these deposits are of Middle Weichselian age, the youngest being 28.5 ka (Salvigsen, 1977). This suggests that the moraines mapped by Liestøl (1972) are of Late Weichselian age. The short distance to the shelf break restricted the extent of the ice sheet westward, and accounts for deposition of the moraines close to the Late Weichselian maximum position. A seismic profile across the shelf off Raudfjorden shows that firm sediments, possibly till, cover the sea floor north of the moraine ridges (A. Solheim, *pers. comm.*, 1996). The higher parts of the outermost islands, Danskøya and Amsterdamøya, are covered by autochthonous block fields interpreted to have been formed on nunataks rising above the surface of the ice sheet (Salvigsen, 1977).

Western Spitsbergen

The west coast of Svalbard is characterised by an alpine mountain range comprised of a belt of pre-Devonian metamorphic rocks. West of the range there is a 5–10-km wide strandflat which continues below the present-day coastline, and the whole continental shelf is ca 60 km wide and less than 200 m deep. Outside the major fjords, the shelf is cut by submarine troughs through which glacial sediment was transported towards large sediment fans on the continental slope (Solheim *et al.*, 1996).

Based on stratigraphic and geomorphologic studies, several researchers (Salvigsen, 1977; Boulton, 1979a; Boulton *et al.*, 1982; Miller, 1982; Forman, 1989; Miller *et al.*, 1989; Lehman and Forman, 1992) have suggested that the Spitsbergen glaciers only experienced a limited advance during the Late Weichselian (see above), filling the inner parts of Kongsfjorden and the tributaries of Forlandsundet and Isfjorden (Fig. 4). This was view partly accepted by Mangerud *et al.* (1987), who suggested a minimum-advance model with restricted ice filling Van Mijenfjorden (Fig. 4), while tidewater glaciers calved along the coasts of Isfjorden during the Late Weichselian. To investigate whether the ice had extended even further west, the land-based studies were followed up by integrated terrestrial and marine investigations along Isfjorden and the adjacent shelf (Svendsen *et al.*, 1989, 1992, 1996; Mangerud and Svendsen, 1990; Mangerud *et al.*, 1992; Elverhøi *et al.*, 1995a). As a result, the maximum position of the reconstructed Late Weichselian ice margin has been moved successively westwards, and the present conclusion is that the glacier extended to the shelf edge off Isfjorden (Fig. 6a,b).

In Kongsfjorden (Figs. 2 and 4), Lehman and Forman (1992) interpreted a moraine lobe close to the mouth to mark a minimum extent of the Late Weichselian glacier. The Late Weichselian marine limit in Kongsfjorden cross-cuts the moraine and is dated to ca 13 ka on its proximal side (Forman *et al.*, 1987). Lehman and Forman (1992), thus, concluded that the ice retreated from the Kongsfjorden moraine ca 13 ka, an idea also supported by an age of 12.3 ka on foraminifera enclosed in glacimarine sediments inside the moraine. Outside the Kongsfjorden moraine, i.e. on Brøggerhalvøya (Fig. 4), two series of raised beaches have been found above the Late Weichselian marine limit. Their partly preserved morphology and lack of

TABLE 1 Key radiocarbon dates associated with the reconstruction of the Late Weichselian ice sheet over Svalbard and the Barents Sea. Most of the dates are plotted as ka in Fig. 3. All dates on marine samples have been corrected for a reservoir age of 440 years (Mangerud and Gulliksen, 1975)

Reservoir corr. age	Lab. ref.	Position	Dated material	Setting	Reference
Western Spitsbergen					
36,100 ± 800	T-5211	78°03′N 13°52′E	*M. truncata*	Beach sediment below till	Mangerud *et al.* (1992)
35,900 ± 500	T-6618	<	< paired	<	<
40,600 ± 1100	T-8184		*M. truncata*	Beach sediment 83 m a.s.l.	<
12,320 ± 190	Ua-729		Shells	Marine sediment above firm diamicton	Mangerud and Svendsen (1990)
12,300 ± 190	Ua-732		Shells	<	<
12,270 ± 110	WHG-531		*E. excavatum*	Marine sediment above till	Lehman and Forman (1992)
12,960 ± 190	B-10967	79°11′N 11°17′E	Whale skull	Beach sediment	Forman *et al.* (1987); Forman (1990)
11,355 ± 125	T-9009	76°43′N 16°20′E	*M. truncata*	Above till	Salvigsen and Elgersma (1993)
41,900 ± 1300	T-9011	76°56′N 16°14′E	<	Below till	<
12,830 ± 210	T-6000	77°34′N 14°24′E	*N. pernula*	Marine above till	Landvik *et al.* (1992a)
12,570 ± 160	Ua-280	<	<	<	<
Shelf west of Svalbard					
14,815 ± 180	TUa-359	78°11.30′N 09°56.56′E	*N. pachyderma*	Marine sediment above firm diamicton	Elverhøi *et al.* (1995a); core NP90-21
14,595 ± 90	TUa-855	<	<	<	<
14,710 ± 120	TUa-856	<	<	<	<
12,545 ± 145	TUa-42	78°02.08′N 12°59.03′E	*Nucula tenuis*	<	Svendsen *et al.* (1992); core NP88-02
19,195 ± 225	Ua-3270	78°14.18′N 08°47.82′E	*N. pachyderma* (sin)	Below debris flow	Andersen *et al.* (1996); core NP90-18C
19,205 ± 205	Ua-3271	<	<	<	<
13,560 ± 120	WHG-941		Benthic foraminifera	Marine above firm diamicton	Lehman *et al.*, *unpublished data*; core NP90-09. Res corr. − 425 years
12,480 ± 121	WHG-946		*N. labradoricum*	<	<
16,440 ± 80	Beta 71988	77°13.20′N 12°37.19′E	*E. excavatum*	Marine sediment above diamicton	Cadman (1996); core NP90-46
14,330 ± 90	Beta 71987	77°17.98′N 12°39.73′E	*E. excavatum/E. asklundi*	<	Cadman (1996); core NP94-4
13,000 ± 70	Beta 78059	<	Shell fragments	<	Cadman (1996); core NP94-4
12,040 ± 80	Beta 81234	77°30.35′N 13°22.04′E	*E. excavatum/C. reniforme*	<	Cadman (1996); core NP90-49
Bjørnøya					
9795 ± 120	Ua-4130	78°28′N 19°02′E	*Bryophyta*	Lake sediment	Wohlfarth *et al.* (1995)
Bjørnøyrenna					
34,835 ± 1430	Ual 052	74°29.4′N 25°46.3′E	Shell fragments	Reworked marine sediment	Hald *et al.* (1990); core 7425/09-U-01
21,615 ± 565	Ual053	<	<	<	<
27,320 ± 735	Ual049	73°16.75′N 23°09.5′E	<	<	Hald *et al.* (1990); core Dia 84-2
21,960 ± 1095	Ual 136	75°19′N 24°43′E	Shell fragments	Diamicton	Elverhøi *et al.* (1993); core 87-21
29,070 ± 1260	Ual 137	<	<	<	<
29,700 ± 925	Ual 138	<	<	<	<
36,160 ± 1900	Ual270	<	<	<	<
42,260 ± 1500	Ua940	<	<	<	<
37,040 ± 900	Ual810	<	<	<	<
24,715 ± 220	TUa-818	74°28′N 10°42′E	Shell	Debris flow deposit	Laberg and Vorren (1995); core JM93-6/1
17,460 ± 145	TUa-820	<	Foraminifera	<	<
Southern Barents Sea					
13,290 ± 290	T-4914	71°25′N 22°54′E	*Macoma calcarea*	Marine sediment	Vorren and Kristoffersen (1986); Vorren and Laberg (1996)

TABLE 1 continued

Reservoir corr. age	Lab. ref.	Position	Dated material	Setting	Reference
Northwest Spitsbergen					
28,530 ± 430,410	T-2091	79°47′N 10°48′E	*M. truncata/H. arctica*	Till	Salvigsen (1977)
38,790 ± 940,840	T-2093	79°42′N 10°49′E	<	Till	<
41,080 ± 2670,2000	T-2094	79°41′N 10°43′E	*H. arctica*	Till	<
9380 ± 110	T-2700	79°35′N 12°45′E	*M. fruncata*	Beach sediment	Salvigsen and Österholm (1982)
43,340 ± 1800,1400	T-2702	79°45′N 13°40′E	*H. arctica*	Beach sediment	Salvigsen and Österholm (1982) (erronously reported in Salvigsen, 1979)
10,050 ± 120	T-2918	79°25′N12°45′E	*M. truncata/H. arctica*	Marine sediment	Salvigsen and Österholm (1982)
11,110 ± 140	T-3099	79°47′N 14°31′E	*M. truncata/H. arctica*	<	<
10,740 ± 190	U-2095	79°55′N18°20′E	*M. truncata*	<	Olsson *et al.* (1969)
10,885 ± 530			Organic	Lake sediment	Karlén (1987)
42,000 ± 3200,2300	T-3294II	80°43′N 20°48′E	*M. truncata*	<	Salvigsen and Nydal (1981)
33,965 ± 630	T-12223	79°43′N 13°10′E	Calcarous algae	Below till	Salvigsen, *unpublished data*
9950 ± 60	T-3100	80°42′N 21°00′E	*H. arctica*	Marine sediment	Salvigsen and Nydal (1981)
Eastern Svalbard					
9850 ± 80	GSC-3039	78°50′N 29°20′E	*Larix* sp.		Salvigsen (1981)
9790 ± 120	T-3397	<	*Larix* sp.		Salvigsen (1981); same as above
10,265 ± 95	Ua-2536	78°34′N 21°20′E	*Nuculana pernula*	Marine above till	Landvik *et al.* (1992b, 1995)
10,330 ± 110	TUa-295	77°59′N 22°59′E	*M. truncata*		<
10,200 ± 95	TUa-269	77°28′N 23°16′E	Shell fragment		Bondevik *et al.* (1995)
Northeast Barents Sea and Franz Josef Land					
13,245 ± 150	TUa-183	79°58.8′N 41°56.9′E	Mixed forams	Marine sediment above diamicton	Polyak and Solheim (1994); core 45
10,150 ± 70	CAMS-5561	80°41.07′N 47°43′E	<	<	Polyak and Solheim (1994); core 45
9990 ± 95	TUa-182	<	<		Polyak and Solheim (1994); core 32
12,890 ± 80	CAMS-5547	81°07.1′N 43°25.92′E	*Cassidulina teretis*		Forman *et al.* (1996); core P1-91-AR-JPC5
11,790 ± 70	CAMS-5548	<	<		< <
10,290 ± 115	GX-17266		*M. truncata*	Marine sediment	Forman *et al.* (1996); Hooker Island, 30 m a.s.l.
10,360 ± 115	GX-17196		Driftwood	Beach sediment	Forman *et al.* (1996); Nansen Island, 27 m a.s.l.
Southeastern Barents Sea					
12,240 ± 135	AA-9452		Mixed foraminifera	Marine sediment above diamicton	
12,525 ± 105	AA-9457		*I. norcossi*	<	Polyak *et al.* (1995); core 305
12,695 ± 115	AA-9458		*I. norcossi*	<	Polyak *et al.* (1995); core 313
12,735 ± 95	AA-12262		Mixed foraminifera	<	Polyak *et al.* (1995); core 313Polyak *et al.* (1995); core 140
Northern Russia					
9779 ± 110	T-11200	67°51′N49°12′E	Peat		Tveranger *et al.* (1995)
9755 ± 150	T-11220	65°15′N52°15′E	Branch of *Salix*		<
10,075 ± 130	T-11219	<	Peat		<

overlying glacial sediments have been taken as evidence that the beaches were not overrun by glaciers during the last glacial maximum (Salvigsen, 1977; Miller, 1982; Forman and Miller, 1984; Forman, 1989). However, Lehman and Forman (1992) showed that well-preserved pre-Late Weichselian beaches also exist on the proximal side of the Kongsfjorden moraine. Even if we do not fully understand the sub-glacial

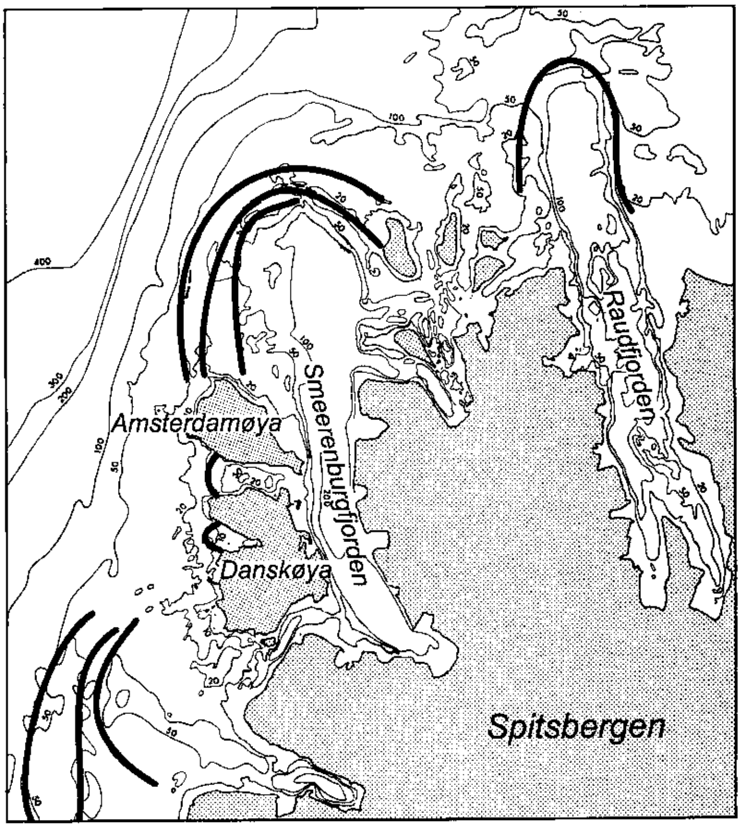

FIG. 5. Submarine moraine lobes off the coast of northwest Spitsbergen (modified from Liestøl, 1972). For location, see Fig. 4.

processes related to the ice sheet, their study demonstrates that glaciers may override beach sediments without either removing them by erosion or depositing any till.

The problem of the ice extent in Kongsfjorden has recently been addressed by Lehman, Solheim, Elverhøi and Jones (*unpublished data*), who retrieved cores from the sea floor of the trough west of the fjord mouth (Fig. 3). They obtained ages of 13.6 and 12.5 ka from marine sediments overlying a firm diamicton interpreted as a till. These ages, thus, suggest that the glacier must have extended beyond the Kongsfjorden moraines and overrun the old beaches on the Brøggerhalvøya peninsula prior to 13.6 ka.

Undisturbed pre-Late Weichselian deposits have also been reported from Prins Karls Forland (Salvigsen, 1977; Troitsky *et al.*, 1979) and from the west coast of Spitsbergen north of Isfjorden (Fig. 2) (Forman, 1989). Based on the evidence for a grounded glacier covering the entire shelf west of Isfjorden (see below) or at least parts of the shelf off Kongsfjorden, we conclude that only some of the highest mountains on Prins Karls Forland could have remained ice free during the Late Weichselian glacial maximum. Seismic profiles and sediment cores show that the sediment succession in the Isfjorden basin continues into Forlandsundet without any thicker sediments beneath (Svendsen *et al.*, 1996). The similarity in sediment and seismic stratigraphy is a strong indication of a similar glacial history for the two areas.

Isfjorden.

Isfjorden, the largest fjord system on Spitsbergen, is 200–400 m deep, and continues across the shelf as the Isfjorden trough (Fig. 4). The fjord may have been filled with a fast-flowing outlet glacier that drained a large portion of the former ice sheet over Spitsbergen during several glaciations. However, Lavrushin (1967, 1969) and Troitsky *et al.* (1979) concluded from studies and ages at Kapp Ekholm and other sections that the Late Weichselian glaciers were not much larger than at present. This conclusion was also supported by an initial study by Mangerud and Salvigsen (1984). Boulton (1979a) also studied the Kapp Ekholm section, and suggested that the Late Weichselian glacier advanced only to the submarine moraine at the mouth of Billefjorden some time between 11 and 10 ka. Subsequently, Mangerud and Svendsen (1992) demonstrated that Late Weichselian ice overran the section at Kapp Ekholm, and that > 30 ka ages reported by Lavrushin (1969) were obtained from glaciotectonically disturbed sediments that were not covered by till in the part of the section studied by Lavrushin. However, a Late Weichselian till occur in other parts of the section.

One main problem in the reconstruction of the Late Weichselian ice margin in Isfjorden has been the lack of a terrestrial record that shows unambiguously ice drainage through the main fjord. A minimum reconstruction of the ice margin, based on till fabric and glacial striae (Mangerud *et al.*, 1987), suggested that

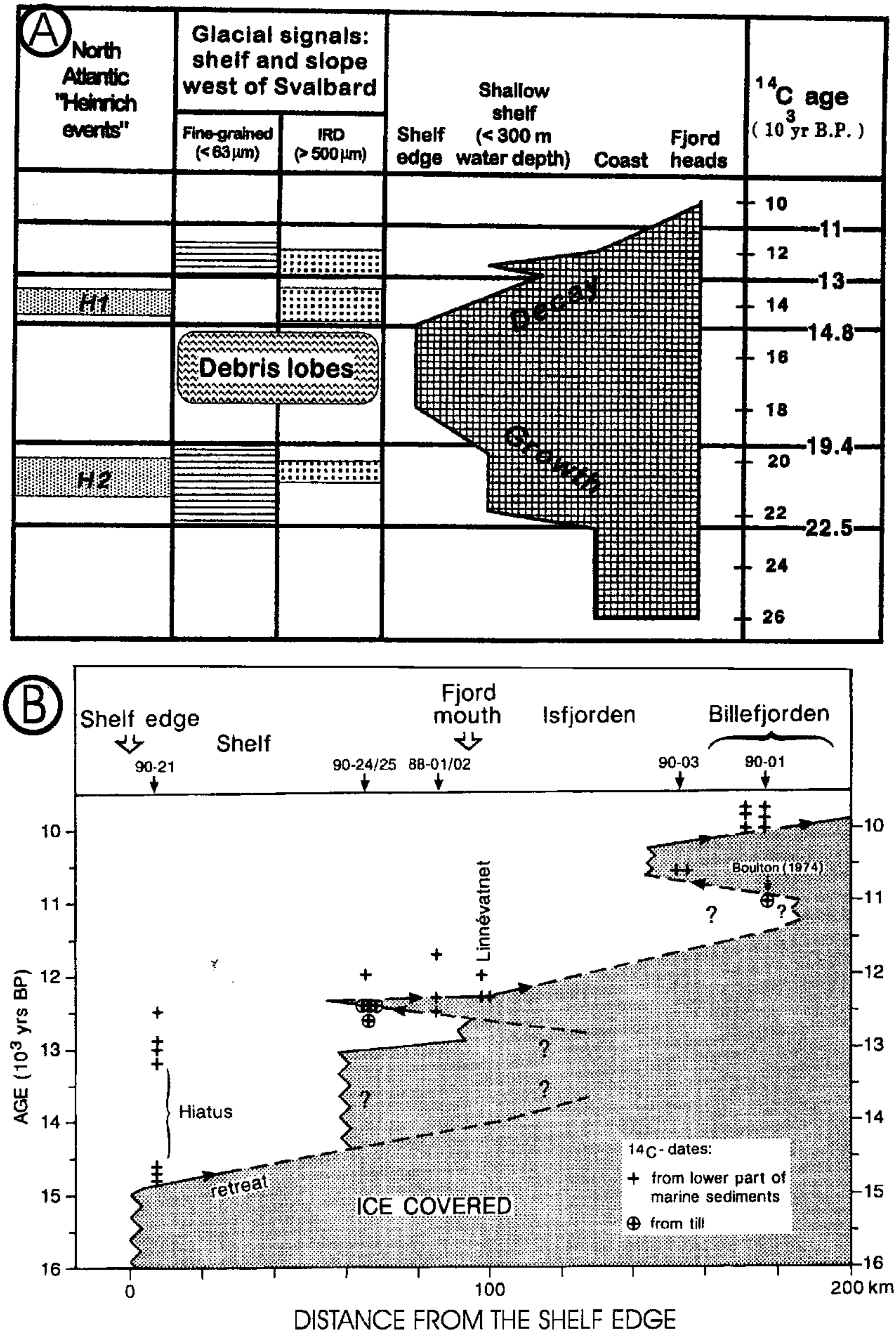

FIG. 6. (A) Glaciation curve from the western Svalbard continental shelf coupled with event mapped in offshore sediment cores (from Elverhøi et al., 1995b). (B) Details of the post 16 ka glaciation on the shelf off Isfjorden (from Svendsen et al., 1996).

valleys and tributary fjords on the north and south sides of Isfjorden were filled with tide-water glaciers that calved along the main fjord. From the stratigraphy in Linnédalen (Fig. 4), the glaciation can be constrained to have occurred somewhere between 25 and 12.3 ka. Raised beach sediments below a till bed yielded radiocarbon ages of 36 and 40.6 ka (Mangerud *et al.*, 1992, 1998). Till fabric analyses show deposition by a glacier moving north down the Linnédalen valley, which runs perpendicular to the main fjord. Amino acid aIle/Ile ratios show that the shells had been covered by ice (0°C) for a maximum of 10,000 years (Mangerud *et al.*, 1992). The valley was deglaciated 12.3 ka (Fig. 3), as shown by basal ages from the sediments in the adjacent Linnévatnet (Mangerud and Svendsen, 1990; Mangerud *et al.*, 1992).

It is interesting to note that the land record in the Isfjorden area can account only for the minimum extent of the Late Weichselian glaciers as suggested by Mangerud *et al.* (1987). However, no observation on land excludes a larger ice extent. Therefore, investigations during recent years have been aimed towards mapping the maximum glacier extent in the fjord basin and the adjacent continental shelf and slope (Mangerud *et al.*, 1992; Svendsen *et al.*, 1992, 1996; Elverhøi *et al.*, 1995a; Solheim *et al.*, 1996). Sea-floor cores along a transect from Isfjorden to the shelf break show a firm diamicton directly overlain by a clayey silty mud with outsized clasts (Mangerud *et al.*, 1992; Elverhøi *et al.*, 1995a; Svendsen *et al.*, 1996). The lateral distribution of the diamicton can be traced on seismic profiles from the main fjord to the adjacent shelf, where it is recorded as an acoustically opaque unit underlying more transparent sediments that become thicker toward Spitsbergen (Svendsen *et al.*, 1992; Elverhøi *et al.*, 1995a; Solheim *et al.*, 1996). The diamicton has been sampled from a set of cores located between the mouth of Isfjorden and the shelf break (Svendsen *et al.*, 1992, 1996). It appears as poorly-sorted homogeneous and slightly over-consolidated sediment with angular to sub-angular, often striated gravel that is derived from the Isfjorden drainage area. Eighteen age estimates on shell fragments from the diarmicton yield ages older than 37 ka (Svendsen *et al.*, 1996). The diamicton could have been formed either by sub-glacial processes, iceberg turbation or debris flows. However, the lithology, the degree of consolidation, lack of stratification and extensive lateral distribution of the diamicton suggest formation as a sub-glacial till.

The thick deposits on the continental slope immediately west of the Isfjorden trough play a key role in our reconstruction of the glacial maximum. The deposits consist almost exclusively of debris lobes (Andersen *et al.*, 1996). Based on AMS radiocarbon ages and oxygen isotope stratigraphy, the uppermost generation of debris lobes correlates with the timing of the last glacial maximum at approximately 18–15 ka. The generation of these features is closely related to the high input of sediments on the upper continental shelf (see Elverhøi *et al.*, 1998; Vorren *et al.*, 1998). As discussed later, the continental slope is in general characterised by low hemipelagic sediment accumulation during that period (Elverhøi *et al.*, 1995a). Thus, high sediment input to the troughs mouth fans, as the one off the Isfjorden trough, is related to direct sediment discharge from a grounded glacier located at the shelf edge (see Vorren *et al.*, 1998). The diamictic composition, including the presence of shallow marine foraminifera in the debris lobes, strongly suggests that this was the mode of deposition for the sediments on the Isfjorden fan.

The seismic stratigraphy across the shelf (Svendsen *et al.*, 1992; Solheim *et al.*, 1996) also indicates an extensive glaciation at a late stage in the geological history. Along the outer shelf between the Isfjorden and Bellsund troughs, the upper units, which have been deposited during the Late Quaternary glaciations (Andersen *et al.*, 1996; Solheim *et al.*, 1996), are truncated by up to 150 m of erosion and a prominent ridge, interpreted to be a terminal moraine, has been formed at the shelf break (Fig. 2). However, these moraines are not radiocarbon dated.

There are three sets of arguments that point to a Late Weichselian age for the till on the continental shelf. A maximum age is given by the > 37 ka dates on shell fragments incorporated in the diamicton. However, and most importantly, four AMS dates from molluscs within the till sampled from two cores from the shelf yielded ages in the range 12.6–12.4 ka, providing strong evidence for an extension of the Late Weichselian ice sheet well beyond the coastline (Svendsen *et al.*, 1996). Svendsen *et al.* (1992) and Svendsen *et al.* (1996) argue that there are no sedimentological signs of a hiatus between the till and the overlying glacimarine sediments. Thus, an ice retreat from the outer shelf at ca 14.8–14.6 ka is concluded from ages on foraminifera and molluscs at the base of the overlying clayey silty mud (Fig. 6b) (Elverhøi *et al.*, 1995a; Svendsen *et al.*, 1996). A further indication of the age at which maximum ice extent was reached at the continental shelf break is provided by two 19.2 ka ages on shells and foraminifera, respectively, below a debris lobe on the Isfjorden Fan (Andersen *et al.*, 1996).

Bellsund

The wide embayment of Bellsund branches eastwards into two major fjords (Fig. 4). Studies on the land around the mouth of the fjord (Landvik *et al.*, 1987, 1992a; Mangerud *et al.*, 1992) led to a reconstruction of a minimum-advance model for the extent of the Late Weichselian ice sheet in which Bellsund acted as a calving bay prior to 12.8 ka. The main evidence for this glacial scenario are: (1) a sub-glacial till showing northerly ice flow on the south coast of Bellsund (Landvik *et al.*, 1992a); (2) deglaciation dates of 12.8 and 12.6 ka on shells from marine clay immediately above the till (Landvik *et al.*, 1992a); and (3) the termination of the 11 ka shoreline at the mouth of Van Mijenfjorden (Landvik *et al.*, 1987; Mangerud *et al.*, 1992).

The stratigraphy on the shelf off Bellsund shows features similar to those found on the Isfjorden shelf (above). In a set of cores from the outer part of the Bellsund trough (Fig. 3), dates of 16.4, 14.3 and 13.0 ka were obtained from sediments overlying a diamicton interpreted as a sub-glacial till (Cadman, 1996). These ages show that the Late Weichselian glacier extended almost to the shelf break, and that deglaciation of the outer part of the shelf started prior to 16.4 ka.

Hornsund and Sørkapp Land

Sub-till sediments occur within a few places. Two glacial phases are represented in a section near Gåshamna on the southern shore of the Hornsund fjord (Fig. 4) (Salvigsen and Elgersma, 1993), where shells below the upper till have yielded ages of about 42 ka (T-9011). Further south, near Olsokbreen, shells above till yielded age estimates of about 11.4 ka (T-9009).

Their position close to the neoglacial lateral moraine of Olsokbreen indicates that the glacier cover over Sørkapp Land was less extensive at 11.4 ka BP than it is today (Salvigsen and Elgersma, 1993). Deglaciation TL and radiocarbon ages of 10–11 ka from this region are also reported by Lindner and Marks (1993).

Western Barents Shelf

The northern and central Barents Sea (Fig. 2) have a generally thin (< 10–15 m) cover of Quaternary sediments above the Mesozoic bedrock (Solheim and Kristoffersen, 1984; Elverhøi *et al.*, 1993). The sediment thickness increases towards the western margin, and may exceed 600 m at the outer parts of the large troughs (Vorren *et al.*, 1992). The general stratigraphy (Fig. 7) consists of a stiff diamicton interpreted as basal till overlain by softer glacimarine sediments deposited during ice recession. At water depths < 100 m, the succession is capped by a thin veneer of fine-grained sediments, which is replaced by reworked sand and gravel on the banks (Elverhøi *et al.*, 1993).

Storfjordrenna, Spitsbergenbanken and Bjørnøyrenna

The major geomorphologic features of the western Barents shelf are the Storfjordrenna and Bjørnøyrenna troughs that are separated by the shallow (< 50 m deep) Spitsbergenbanken (Fig. 2). Bjørnøyrenna, the larger of the two troughs, is ca 750 km long and stretches from Storbanken to the shelf break. It reaches almost 500 m water depth south of Bjørnøya. Storfjordrenna is smaller and separates the shallow Spitsbergenbanken from the main islands of Svalbard to the north (Fig. 2). The Bjørnøyrenna trough mouth fan, which extends from the mouth of Bjørnøyrenna into the deep sea, is the largest depositional feature on the Barents Sea margin (Vorren *et al.*, 1998). The large

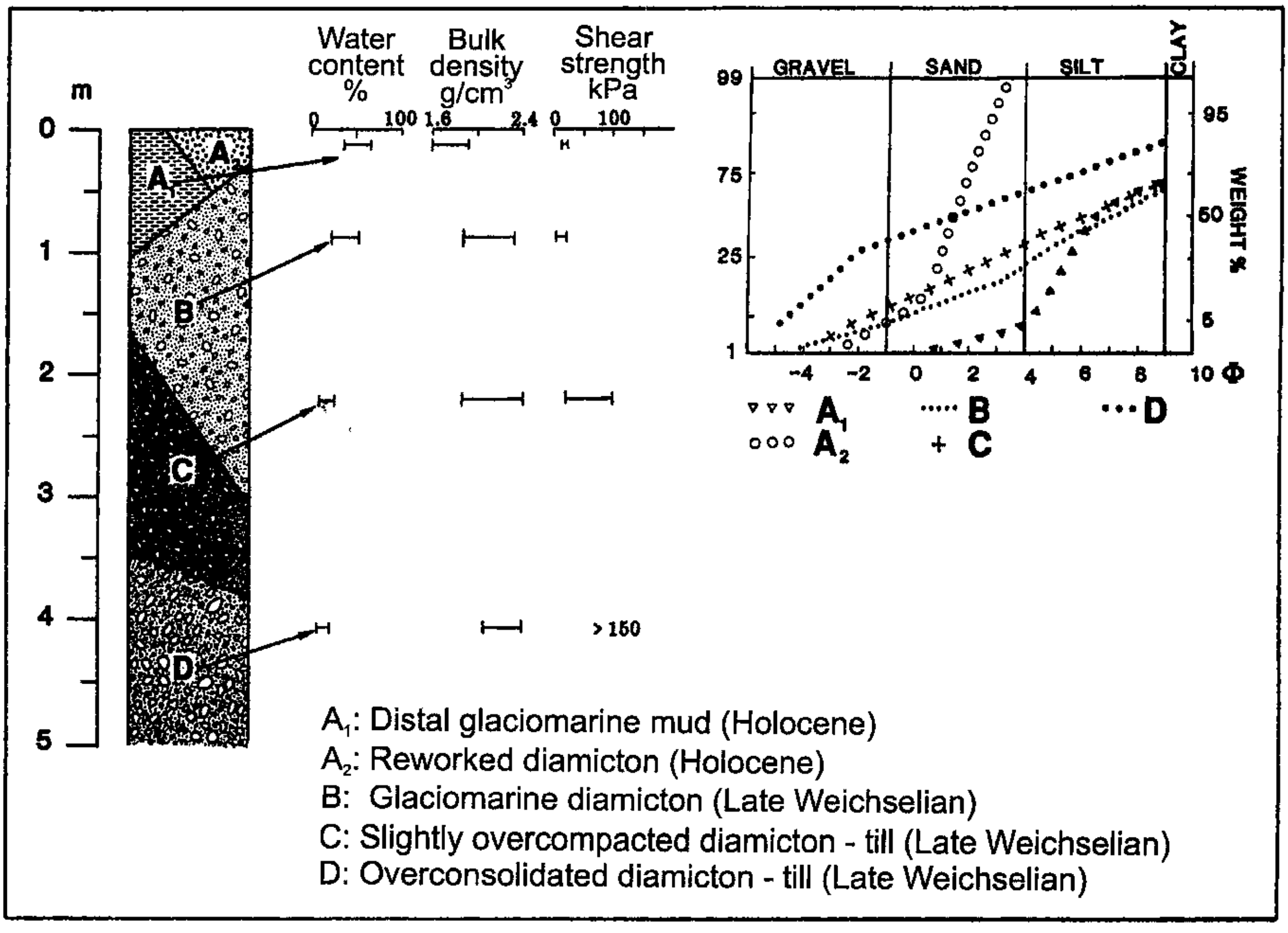

FIG. 7. General lithostratigraphy for the central and northern Barents Sea (after Elverhøi *et al.*, 1993).

volumes of glacigenic sediments are evidence that the troughs may have acted as major ice drainage pathways for successive Barents Sea glaciations (Laberg and Vorren, 1995; Vorren and Laberg, 1996).

Several glacial features within the two troughs have been used to reconstruct the Late Weichselian ice distribution (see Elverhøi *et al.*, 1993). A set of 20–50 m high sediment ridges are found at 300 m depth along the western and southern margins of Spitsbergenbanken (Fig. 2) (Elverhøi and Solheim, 1983a,b; Solheim and Kristoffersen, 1984). The ridges were interpreted as moraines (Elverhøi and Solheim, 1983a) and correlated to large bodies of acoustically transparent ice proximal sediments occurring at the same depth both at the mouth of Storfjordrenna and in the inner part of Bjørnøyrenna (Fig. 2) (Elverhøi *et al.*, 1990, 1993).

In the southern Barents Sea, Vorren and Kristoffersen (1986) identified marginal moraines some of which were deposited from the northeast, i.e. from an ice sheet located in the southern Barents Sea, evidently also occupying Bjørnøyrenna. The most convincing evidence that a grounded glacier existed in Bjørnøyrenna is the discovery of large areas containing 100–500-m long parallel linear groves and ridges, interpreted as subglacially formed flutes (Solheim *et al.*, 1990). The flutes have been mapped with side-scan sonar both at the head of Bjørnøyrenna, between Spitsbergenbanken and Storbanken, and in a smaller area in the central part of the trough south of Spitsbergenbanken (Fig. 2). The latter site shows that the ice extended beyond the moraines discussed above. The flutes are developed at the surface of the firm mud which is interpreted as a till (Solheim *et al.*, 1990), and in several large areas they are covered by a thin veneer of post-glacial sediments. The stratigraphic position and the thin, or absent, sediment cover are strong evidence supporting a Late Weichselian age of the till.

As discussed for Isfjorden west of Svalbard, the thick debris lobes in the Bjørnøyrenna trough mouth fan play a key role in the understanding of the western extent of the Late Weichselian ice sheet (see Vorren *et al.*, 1998). Seismic studies suggest that the fan was constructed mainly by large-scale debris flows which formed by down-slope movement of sediments brought to the shelf break by glaciers (Solheim and Kristoffersen, 1984; Vorren *et al.*, 1989; Laberg and Vorren, 1995). Radiocarbon age estimates on foraminifera in the uppermost debris lobe suggest that deposition occurred after 17.5 ka, i.e. during the Late Weichselian (Laberg and Vorren, 1996; Vorren and Laberg, 1996). Thus, the glacier must have been grounded at ca 500 m water depths at the mouth of Bjørnøyrenna.

Maximum ages for the onset of the Late Weichselian glacier advance in Bjørnøyrenna have been obtained from a set of five sediment cores in a transect from Spitsbergenbanken in the north to Fugløybanken in the south (Fig. 3). In the central parts of Bjørnøyrenna (cores 7425/09-U-01 and DIA 84-2), Hald *et al.* (1990) reported radiocarbon ages of 34.8, 27.3 and 21.6 ka, obtained from reworked shells in marine sediments (Table 1; Fig. 3). Similarly, on the margin of Spitsbergenbanken, south of Hopen (core 87–21), Elverhøi *et al.* (1993) obtained six ages on shell fragments between 42.3 and 22.0 ka in a diamicton interpreted as till (Table 1; Fig. 3). In a core (core JM93-6/1) penetrating the distal parts of one of the debris lobes on the trough mouth fan, Laberg and Vorren (1995) dated foraminifera and molluscs incorporated in the debris lobe diamicton to 17.5 and 24.7 ka. (Table 1; Fig. 3). From these ages we conclude that the glacier advanced through Bjørnøyrenna some time after ca 22 ka, as suggested by Elverhøi *et al.* (1995b) (Fig. 8).

Bjørnøya

The island of Bjørnøya (Figs. 1 and 2) lies close to the western margin of the Barents shelf and, thus, close to the margin of any former ice sheets in the Barents Sea. From findings of glacial erratics and striae, it has been known for almost a century that the island once was covered by glaciers (Nathorst, 1899; Horn and Orvin, 1928). A re-investigation of the glacial geology of the island was carried out by Salvigsen and Slettemark (1995). They found that the erratics were solely derived from the local bedrock, and concluded that the numerous glacial striae (Salvigsen and Slettemark, 1995) were formed by a local ice cap. The highest mountains may have been nunataks at this time. A local deglaciation of 9.8 ka is inferred from ages on mosses from basal lake sediments on the northern part of the island (Wohlfarth *et al.*, 1995).

An important question is whether Bjørnøya has been subjected to glacio-isostatic depression as a result of the ice load over the Barents Sea. Earlier reports of raised beaches on Bjørnøya (Horn and Orvin, 1928) were rejected by Salvigsen and Slettemark (1995), who found undisturbed till down to the present day beach.

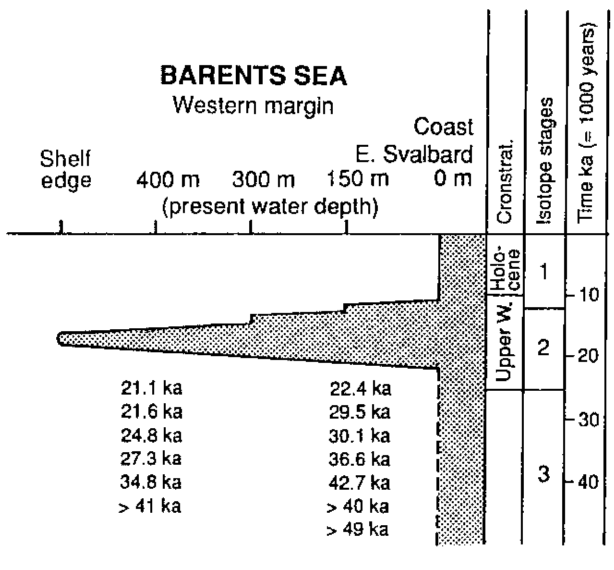

FIG. 8. Glaciation diagram from Bjørnøyrenna (modified from Elverhøi *et al.*, 1993).

We thus conclude that the present sea level represents the post-glacial marine limit on the island. This is also indicated by the southward extrapolation of the 10 ka shoreline that is mapped along the coast of Spitsbergen (Fig. 11) and the isostatic modelling discussed below.

Southern Barents Sea

Reconstruction of the Late Weichselian ice margin in the southern Barents Sea is more complicated than of that farther north, as it represents a confluence zone between the dynamically independent Barents Sea and Fennoscandian ice sheets. From studies on Andøya (Vorren *et al.*, 1988) and the seismic stratigraphy in outer Bjørnøyrenna (Laberg and Vorren, 1995; Vorren and Laberg, 1996) suggested that the last glacial maximum in the southwestern Barents Sea occurred in two phases: the first advance prior to 22 ka, and the later after 19 ka. In our reconstruction we focus on the last advance.

Evidence of grounded ice is found in the southwestern Barents Sea where a system of 10–50-m high and 1–5-km wide moraines were formed in front of lobes from both the Fennoscandian and the Barents Sea ice sheets (Vorren and Kristoffersen, 1986) (Fig. 2). A deglaciation age of 13.3 ka (Fig. 3) from material on the proximal side of the moraine lobes shows that they were formed by the Late Weichselian ice sheet (Vorren and Kristoffersen, 1986). Large-scale glaciotectonic features have also been reported 50–80 km farther west of the lobes (Fig. 2) (Sættem, 1990). These are not dated, but a limited cover of postglacial sediments in the depressions suggests that they were also formed during the Late Weichselian. If this is correct, the ice sheet also extended almost to the shelf break in this region. Thus, the glacier margin inferred by Laberg and Vorren (1995) at the mouth of Bjørnøyrenna (above) may have continued southwards along the shelf break until it met ice flowing off northern Scandinavia (Fig. 12).

Northern Svalbard and the adjacent shelf

Compared with the shelf west of Svalbard and the Barents Sea, less is known about the part of the shelf that faces the Arctic Ocean to the north (Fig. 2). The northern shelf is cut by several large troughs, from the Hinlopen Trough (Fig. 4) in the west to the large Franz Victoria Trough west of Franz Josef Land (Fig. 2).

Northern Spitsbergen and Nordaustlandet

As discussed above, the marine record from the shelf indicates that the Late Weichselian ice extended north of the moraines mapped by Liestøl (1972) and Salvigsen (1977) in the Raudfjorden and Liefdefjorden area. In Mosselbukta (Fig. 4), shells from 65 m a.s.l. were dated to 11.1 ka, while the upper marine limit was determined to 85 m a.s.l. (Salvigsen and Österholm, 1982). This elevation of the marine sediments is comparable with the situation on the west coast of Svalbard, between Isfjorden and Van Mijenfjorden, where it has been shown that the Late Weichselian ice sheet extended to the shelf break. Thus, we suggest that a substantial isostatic load existed over the north coast, and that the Late Weichselian ice sheet extended to an unknown position on the continental shelf to the north.

Radiocarbon ages from the western part of Nordaustlandet (Fig. 2) are similar ages obtained from Mosselbukta. The minimum age for the deglaciation in the Murchisonfjorden area (Fig. 4) is demonstrated by 10.7 ka old shells found 82 m a.s.l. (Olsson *et al.*, 1969). Although the northward extension of the Late Weichselian ice sheet along the north coast of Nordaustlandet is not known, Österholm (1990) argued that because the postglacial marine limit is about 50 m a.s.l. on Prins Oscars Land (Fig. 4), then the Late Weichselian ice sheet extended only to the coast line. Deglaciation ages older than 10 ka have not been obtained from the north coast of Nordaustlandet, but Österholm (1990) suggested that deglaciation took place about 11 ka or earlier. Investigations on Sjuøyane (Fig. 4) (Salvigsen and Nydal, 1981) led to the conclusion that the Late Weichselian ice sheet did not reach Sjuøyane. The marine limit there was determined to be 22 m a.s.l. The isobase map (Fig. 9) indeed indicates that the Late Weichselian ice sheet reached at least Sjuoyane. Shells found above the marine limit as well as shells from the upper unit of a sea-facing cliff were dated to > 40 ka, whereas shells of 10 ka indicate a minimum age of the deglaciation (Salvigsen and Nydal, 1981).

Franz Victoria Trough and Franz Josef Land

Two independent studies of sediment cores from the Franz Victoria Trough at ca 80°N (Polyak and Solheim, 1994) and 81°N (Lubinski *et al.*, 1996) show a typical deglaciation succession of glacial diamictons (tills) overlain by laminated mud. Radiocarbon ages immediately above the diamictons indicate deglaciation prior to 12.9 and 13.2 ka (Fig. 3). Seismostratigraphic studies (Lubinski *et al.*, 1996) demonstrate a large lateral extent of the diamicton, and support the interpretation that it represents a basal till. Thus, the ice was grounded down to a modem water depth of ca 400 m. Seismic studies as far north as 81.5°N also suggest that the sea floor in the outer parts of the trough is covered by the same till bed (A. Solheim, *pers. comm.*, 1996), which supports Late Weichselian ice grounded within most of the Franz Victoria Trough down to a modem depth of ca 500 m.

The Franz Josef Land archipelago represents the northernmost islands on the Barents Shelf (Fig. 1). They have low relief with adjacent shallow banks cut by the 500–600 m deep Franz Victoria Trough to the west, and the large 600–700 m deep Svayataya Anna Trough to the east (Fig. 2). As with other islands in the

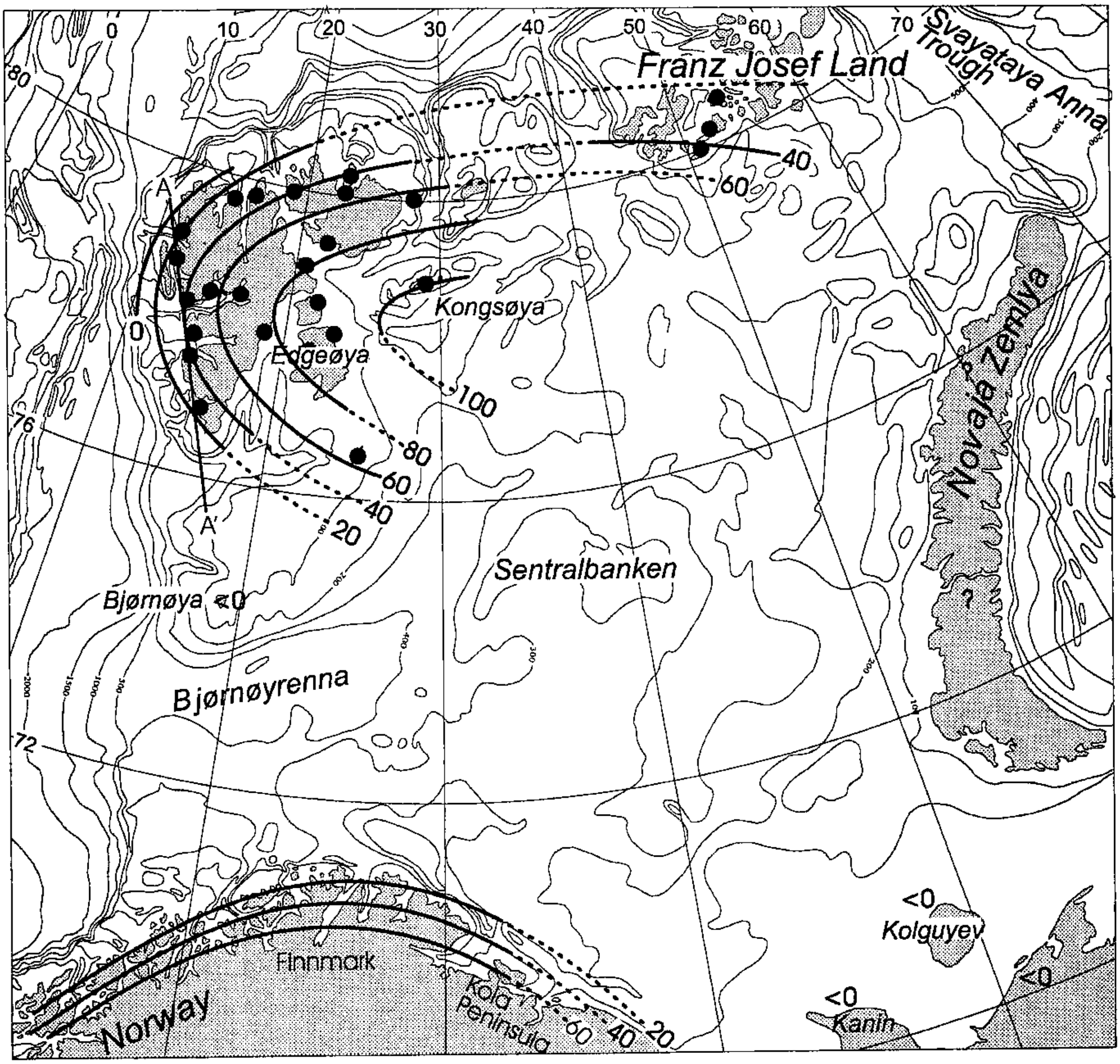

FIG. 9. Isobases showing the 10 ka shoreline for the land areas bordering the Barents Sea. The map is constructed from available sea level curves (dots) and independent determinations of the 10 ka level. The following data sources have been used: isobases over Svalbard from Bondevik *et al.* (1995); sea levels on Franz Josef Land from Forman *et al.* (1996); data from northern Norway from Sørensen *et al.* (1987) and towards the Kola Peninsula from Marthinussen (1974); and further east from Svendsen, Astakhov and Mangerud (*unpublished data*).

region, previous studies have suggested limited glaciation during the Late Weichselian (see review by Forman *et al.*, 1996). However, recent studies on several of the south-central islands reveal a glacial diamicton overlying bedrock, succeeded by offlapping beach sequences up to a marine limit that drops from 50 m a.s.l. in the north to ca 30 m a.s.l. in the south (Forman *et al.*, 1996). Ages on driftwood and *in situ* molluscs close to the marine limit indicate a deglaciation 10.3–10.4 ka (Forman *et al.*, 1996), whereas deglaciation dates in marine cores in one of the western fjords suggest they were deglaciated by 10.0–10.2 ka. (Polyak and Solheim, 1994). There are no geological observations that help constrain the ice extent on the continental shelf north of Franz Josef Land. However, shorelines as high as 50 m a.s.l. indicate a relatively thick ice cover and, thus, that the ice margin was situated some distance offshore.

Eastern Barents Sea

Novaja Zemlya and the adjacent sea

Seismostratigraphic and sediment-core studies (Gataullin *et al.*, 1993) have shown that the sea floor west of Novaja Zemlya is characterised by an extensive diamicton layer (seismostratigraphic unit III) overlain by glacimarine and postglacial sediments. The diamicton has characteristics of a true till, and contains inclusions of unlithified Mesozoic sediments, striated clasts and redeposited pre-Quaternary foraminifera and palynomorphs. The surface of the diamicton is irregular and rough, a morphology attributed to iceberg ploughing (Gataullin *et al.*, 1993). Because the unit rests directly on the upper regional unconformity (URU) in the area, considerable erosion must have taken place during the Late Weichselian. Thus, no maximum age has been obtained for the deposition of the till. Prominent arc-shaped morainic ridges up to 100 m in relief are found west of Novaja Zemlya (Fig. 2) (Epshtein and Gataullin, 1993). Evidently, these end moraines reflect ice dispersal from the east, and they were possibly deposited along the margin of an ice sheet that was centred in the Kara Sea. The age of these moraines is unknown, but their fresh morphologies suggest a Late Weichselian age. This is supported by the fact that on the distal side of the moraines, deposition of glacimarine sediments upon till began shortly before 12.7 ka (Fig. 3) (Polyak *et al.*, 1995). Thus, grounded ice must have extended west of the ridges. On Novaja Zemlya there are few radiocarbon ages from well-documented stratigraphic contexts that can be directly related to a Late Weichselian glaciation.

The north Russian coast

The present knowledge of the extent and timing of the Kara Sea Ice sheet on the European part of the Russian mainland is based partly on preliminary results obtained by the ongoing Russian–Norwegian research project PECHORA (Paleo Environment and Climate History of the Russian Arctic) (see review in Rutter, 1995). On the basis of the end moraine configuration, till fabrics, erratics, striations and other ice-directional features, it has been known for some time (Astakhov, 1979) that the youngest ice flow that affected the Pechora basin (Fig. 1) is from the northeast (reviews in Grosswald, 1993; Astakhov, 1994; Punkari, 1995). Thus, there is good evidence to suggest that the last ice sheet inundating the coastal areas to the east of the Kanin Peninsula (Fig. 2) was dynamically connected with the Kara Sea ice sheet and not the Barents Sea ice sheet. However, the Kara Sea ice sheet must have merged with both the Fennoscandian and the Barents Sea ice sheets in the southeastern Barents Sea, provided that they existed at the same time.

The extent and timing of the last glaciation of European arctic Russia is controversial. According to Grosswald (1993) the Late Weichselian ice sheet extended several hundred kilometres to the south of the present coast line. However, based on recent investigations in the Pechora Basin it has been concluded that the Weichselian glaciation was much less extensive than Grosswald predicted (Tveranger *et al.*, 1995). The latter researchers suggest that the Weichselian glacial maximum corresponds with the so-called Markhida Moraine, a broad zone of ice-marginal landforms running east-west across the Pechora lowland (Fig. 2). Grosswald (1993) concluded that this end moraine was formed during a re-advance of the Kara ice sheet after 9 ka. However, Tveranger *et al.* (1995) demonstrated that the postulated young ice advance was due to a misinterpretation of the sediments and stratigraphy, and that the Markhida Moraine is older than 10 ka. Based on TL dates that were obtained from fluvial sediments under till, they tentatively suggested a Late Weichselian age for the formation of the end moraine. However, this has not yet been confirmed by radiocarbon ages.

Alternatively, the last ice advance that reached the Markhida Moraine occurred during the Middle or Early Weichselian.

HOLOCENE RELATIVE SEA LEVEL

The pattern of glacio-isostatic uplift has been a widely used tool used to reconstruct Late Weichselian ice sheets in different arctic regions. Modelling of the Earth's response to glacial loading has been one of the few methods available for reconstructing the spatial configuration of past ice sheets, as has been done for the former ice sheet over the Barents Sea (Elverhøi *et al.*, 1993; Lambeck, 1995, 1996; Breuer and Wolf, 1995).

Schytt *et al.* (1968) first published an isobase map based on the elevation of a mid-Holocene pumice horizon, indicating a centre of uplift in the northern Barents Sea. Later, a 9.8-ka-old driftwood log found in beach sediments 100 m. a.s.l. on Kongsøya (Fig. 2) demonstrated that this uplift was caused by melting of a large Late Weichselian ice sheet over the northern Barents Sea and Svalbard (Salvigsen, 1981). Such an uplift centre over the northern Barents Sea was also shown by the 5 ka isobase map constructed from recent data by Forman *et al.* (1995).

An isobase map based on the elevation of shore lines formed just after the deglaciation would depict the load of glacier ice better than isobase maps constructed for younger periods. Deglaciation ages suggest an almost instantaneous and final withdrawal of the last ice sheet from the land areas bordering the Barents Sea at ca 10 ka (Fig. 3). We have, therefore, constructed an isobase map for 10 ka for the Barents Sea region (Fig. 9).

Observations

Sequences of raised beaches are common on the forelands bordering the Barents Sea (Fig. 10) (e.g. Marthinussen, 1974; Salvigsen, 1978, 1981; Forman, 1990; Bondevik *et al.*, 1995; Forman *et al.*, 1996). Dating of the raised beaches has provided data sets for construction of isobase maps. Our reconstruction (Fig. 9) is based on 24 independent relative sea-level curves from the Svalbard archipelago, in addition to local determinations of the marine limit and data from Franz Josef Land (Glazovskiy and Näslund, 1992; Näslund

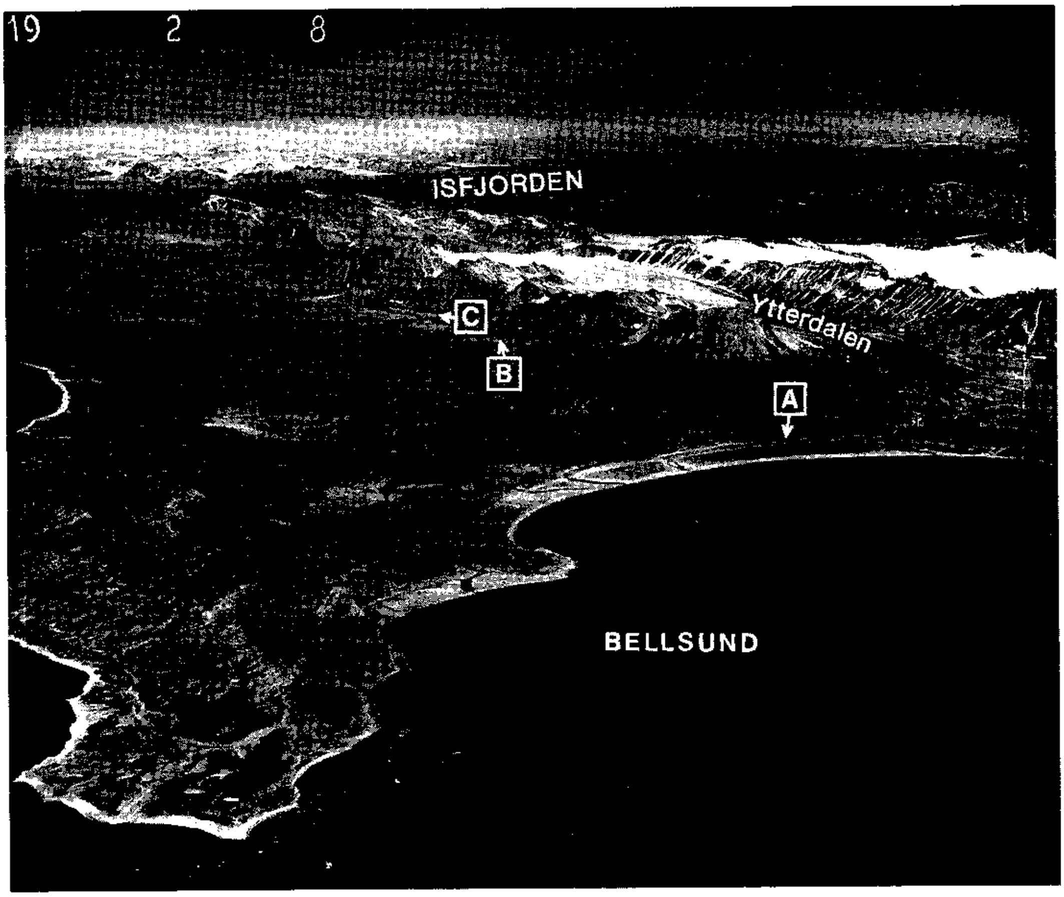

FIG. 10. Examples of raised beaches on Svalbard. Oblique air photograph of Nordenskiöldkysten seen from Bellsund. The three main beach levels are shown: the Tapes transgression beach ridge (A); the 10 ka shoreline (B); and the marine limit (C). Photograph: Norsk Polarinstitutt S 36 1928.

et al., 1994; Forman *et al.*, 1996) and from the coast of northern Norway eastwards to the Kola Peninsula (Sollid *et al.*, 1973; Marthinussen, 1974; Snyder *et al.*, 1996).

Svalbard

The west coast of Svalbard was deglaciated between 13 and 12 ka, and at about 10 ka, the glaciers had receded to the head of all fjords (Mangerud *et al.*, 1992). Some of the shore lines formed prior to 10 ka are broad (50–100 m) beach ridges or spits formed by long-shore drift (Forman *et al.*, 1987; Landvik *et al.*, 1987; Forman, 1990). Radiocarbon age estimates of shells and whale bones indicate a slow emergence, or even still-stand, during the formation of these shorelines (Fig. 11). A prominent beach ridge that is found along the west coast is informally named beach level B by (Landvik *et al.*, 1987) (Fig. 10). Most radiocarbon ages indicate an age between 10.6 and 10.0 ka. Beach level B probably indicates a transgression or a stable sea level during parts of the Younger Dryas (Landvik *et al.*, 1987). We have used the elevation of this beach to map the 10 ka isobase in a north-south profile along the west coast (Fig. 11).

Both the marine limit and the 10 ka shoreline show a distinct updoming around the central part of Spitsbergen, i.e. the Isfjorden–Van Mijenforden area (Fig. 11). The northwestern tip of Spitsbergen is characterised by little post-glacial emergence, and the Late Weichselian marine limit here is probably close to the present sea level (Lehman and Forman, 1987) (Figs. 9 and 11). At Bjørnøya, at the southern end of the profile in Fig. 11, no raised shorelines are found (Salvigsen and Slettemark, 1995). The local deglaciation is dated to 9.8 ka (Wohlfarth *et al.*, 1995), and by extrapolation of the 10 ka shoreline in Fig. 11, we estimate that relative sea level at Bjørnøya was about 40 m below present at the time of the local deglaciation.

Due to the large amount of well-preserved driftwood on the raised beaches in eastern Svalbard, relative sea-level curves from this area are much better constrained than on western Svalbard (Salvigsen, 1978, 1981; Bondevik *et al.*, 1995). The marine limit was formed about 10 ka in large parts of central eastern Svalbard, following a rapid deglaciation of the area at this time (Landvik *et al.*, 1995). Subsequently, the whole archipelago started to emerge rapidly (Salvigsen, 1981; Forman, 1990; Bondevik *et al.*, 1995).

Franz Josef Land

Several relative sea-level curves have been constructed from the islands in the Franz Josef Land archipelago (Fig. 9) (Glazovskiy and Näslund, 1992; Näslund *et al.*, 1994; Forman *et al.*, 1996). Forman *et al.* (1996)

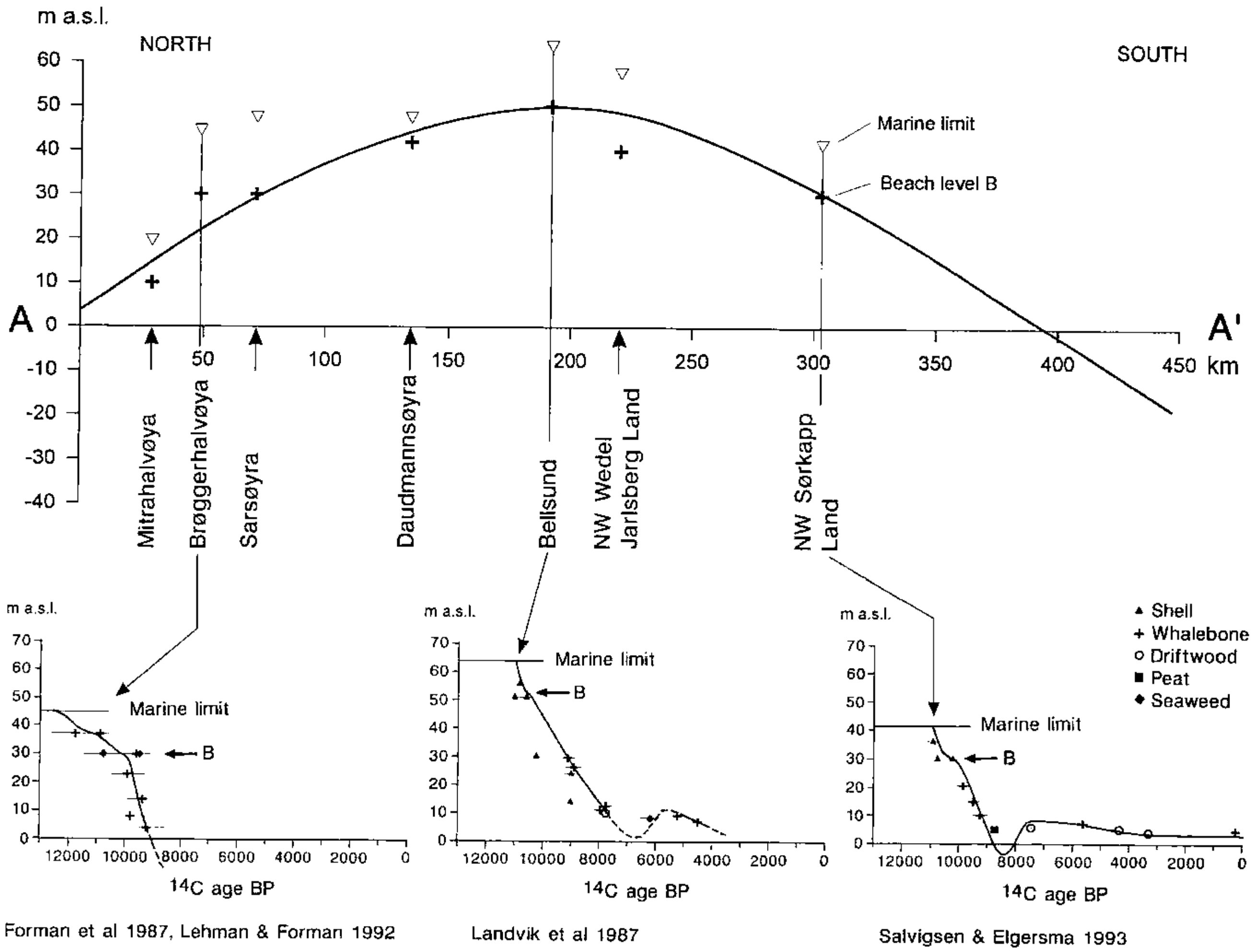

FIG. 11. North–south profile of the marine limit and beach level B (10 ka) along the west coast of Svalbard. The sea-level curves from three selected locations are shown. The profile is located on Fig. 9.

dated the deglaciation to ca 10 ka (Fig. 3), and found that the elevation of the marine limit increases towards the Barents Sea, from 25 m a.s.l. in the northeast, to almost 50 m a.s.l. in the southwest (Fig. 9). This increase indicates that the archipelago and adjacent shelf were subjected to ice loads similar to that on the western part of Svalbard.

Novaja Zemlya

Grosswald (1980) reported postglacial marine terraces > 100 m a.s.l. However, Forman *et al.* (1995) concluded that the post-glacial marine limit on northwestern Novaja Zemlya was formed by a transgression ca 6 ka and is less than 20 m a.s.l. They also interpreted the higher beaches to be covered by discontinuous glacial drift, and that they are, thus, of a pre-Late Weichselian age. Based on both minimum and maximum ice extent models, Lambeck (1995) calculated a 10 ka marine limit to be 60 and 250 m, respectively, and concluded that the low marine limits observed could only be explained by a local deglaciation as late as 6 ka. Novaja Zemlya is presently emerging 2 mm/year (Emery and Aubrey, 1991). Such a rate is similar to other regions with a high marine limit (e.g. eastern Svalbard, Bondevik *et al.*, 1995), and suggests strongly that the island was subjected to a considerable glacial load during the last glaciation.

Northern Norway to the Kola Peninsula

Along the northern coast of Norway towards the Kola Peninsula, the isobases run parallel to the coast line (Marthinussen, 1974; Møller, 1987; Snyder *et al.*, 1996), showing that the pattern of the postglacial shorelines in Finnmark was mainly determined by the Fennoscandian ice sheet. However, the shoreline gradients along the Finnmark coast decrease towards the east (Fig. 9), indicating that the load of the Barents ice sheet had some influence on the isostatic uplift in eastern Finnmark (Møller, 1987; Elverhøi *et al.*, 1993; Lambeck, 1995).

Mainland Russia and east of the White Sea

Along the coast of the Pechora lowland, Arslanov *et al.* (1987) described a terrace 15–17 m a.s.l., which they interpreted to be of early Holocene age. However, during recent fieldwork, Mangerud *et al.* (1993a, b) and Svendsen *et al.*, (*unpublished data*) found that the sediments are of continental origin (lacustrine and eolian), and that there are no marine terraces and sediments along that coast. In a review of the Russian literature, Astakhov (1994) concluded that there are no raised shorelines on Cape Kanin or the Kolgujev Island (Fig. 9). The conclusion is that all Late Weichselian and Holocene shore lines are below the present sea level along the southeast coast of the Barents Sea. Thus, the isobases in northern Norway and the Kola Peninsula (Fig. 9) turn south into the White Sea and encircle the Scandinavian ice sheet. Any possible Late Weichselian ice sheet in the southeastern Barents Sea did not significantly influence the isostatic emergence pattern of the Kola Peninsula and northern Norway after ca 12 ka.

Configuration of the emergence patterns

The 10 ka isobase map (Fig. 9) shows two independent domes, a Svalbard–northern Barents Sea dome and a Fennoscandian dome. The Svalbard–Barents Sea emergence dome shows a well-defined elliptical configuration. The largest observed emergence is on Kongsøya and the tilt of the isobases points towards a centre of uplift south east of Kongsøya (Fig. 9). The largest uncertainty is still the continuation of the isobases towards Novaja Zemlya. Even if the deglaciation of the west coast of the island is dated to ca 10 ka (Forman *et al.*, 1995), no raised beaches from this period have been found. Based on their reconstruction of the 5 ka isobases, Forman *et al.* (1995) suggested that the uplift of Novaja Zemlya was mainly influenced by the Kara Sea ice sheet.

Implications for the last glacial maximum ice sheet

The reconstructed emergence domes reflect mainly the ice thickness just prior to the major unloading/deglaciation. The isobase map shows an elliptic dome that reflects a maximum iceload over northern Barents Sea at that time (Fig. 9).

The relative sea-level curves for the region (see Fig. 11) show that half of the emergence was completed within 2000 years after the local deglaciation. Thus, an isostatic signal from the deglaciation of the central or southern part of the Barents Sea at 15–14 ka might be hard to detect. By the time the land areas bordering the Barents Sea were deglaciated, 50–75% of the isostatic emergence in the central Barents Sea may have been completed.

This rapid crustal response to unloading is probably the main reason why the isobase pattern constructed from land areas that were deglaciated ca 10 ka, fails to detect rebound from the ice that existed over the southern Barents Sea. However, Bondevik *et al.* (1995) pointed out the possibility that the higher uplift rates on Hopen and southern Edgeøya during the last 7000 years as compared with uplift rates at locations farther north, may be partly a result of rebound from ice load in the southern Barents Sea. Møller (1987) and Lambeck (1995) suggested that the less steep shorelines in eastern Finnmark compared with those further west could have been caused by the same effect.

THE LAST GLACIATION COMPILATION

Our reconstruction of the Late Weichselian maximum ice limit based on the available geological data is shown in Fig. 12. Along the coast of northern Norway, the ice margin of the Fennoscandian ice sheet follows the reconstruction by Vorren and Laberg (1996). The margin lies on the outer shelf, with smaller lobes caused by drainage from the major fjords and troughs. The margin also runs across the northern part of Andøya where lake basins show ice-free conditions from ca 22 ka (Vorren *et al.*, 1988; Alm, 1993). However, the Late Weichselian ice sheet inundated these lakes prior to 22 ka.

Immediately north of the Norwegian coast, ice flowing off the Fennoscandian ice sheet met with ice from the Barents Sea. A minimum extent reconstruction of the ice margin in this convergence zone is shown by the moraines mapped by Vorren and Kristoffersen (1986) (see Vorren and Laberg, 1996). However, it is possible that the moraines only represent a stage during ice retreat. The presence of large glaciotectonic structures at the sea floor further west Sættem, 1990 suggests that the ice sheet extended almost to the shelf break during the Late Weichselian (Fig. 12). According to Vorren and Laberg (1996), there were two major ice advances during the Late Weichselian in the area: LGM I (before 22 ka) and LGM II (after 18 ka). Possibly the ice sheet reached the outermost position during LGM II, and the mapped moraines were deposited during LGM I.

As discussed above, ice filled the Bjørnøyrenna trough out to the shelf break (Solheim *et al.*, 1990; Laberg and Vorren, 1995). Bjørnøya, which sits on a topographic high close to the shelf edge, was ice covered at the same time (Salvigsen and Slettemark, 1995). Glacial striae on the island may indicate that Bjørnøya was covered by a local ice dome, which must have been confluent with the Barents ice sheet during the Late Weichselian. The persistent ice flow off the Bjørnøya topographic high shows that the Barents ice sheet was rather thin close to its margin. Such a model of confluence between ice sheets over Bjørnøya/Spitsbergenbanken with the Barents ice sheet is also supported by a series of recessional moraines on the south slope, and moraines close to the shelf break west of Spitsbergenbanken (Elverhøi *et al.*, 1993) (Fig. 2). Alternatively, the mapped ice movements on Bjørnøya may stem from a late stage of the deglaciation.

Radiocarbon-dated sediment cores containing glacial diamictons along the Spitsbergen shelf (Mangerud *et al.*, 1992; Svendsen *et al.*, 1992, 1996; Cadman, 1996) Lehman *et al.*, *unpublished data*) (Fig. 3) clearly illustrate that glaciers reached the shelf break off the major

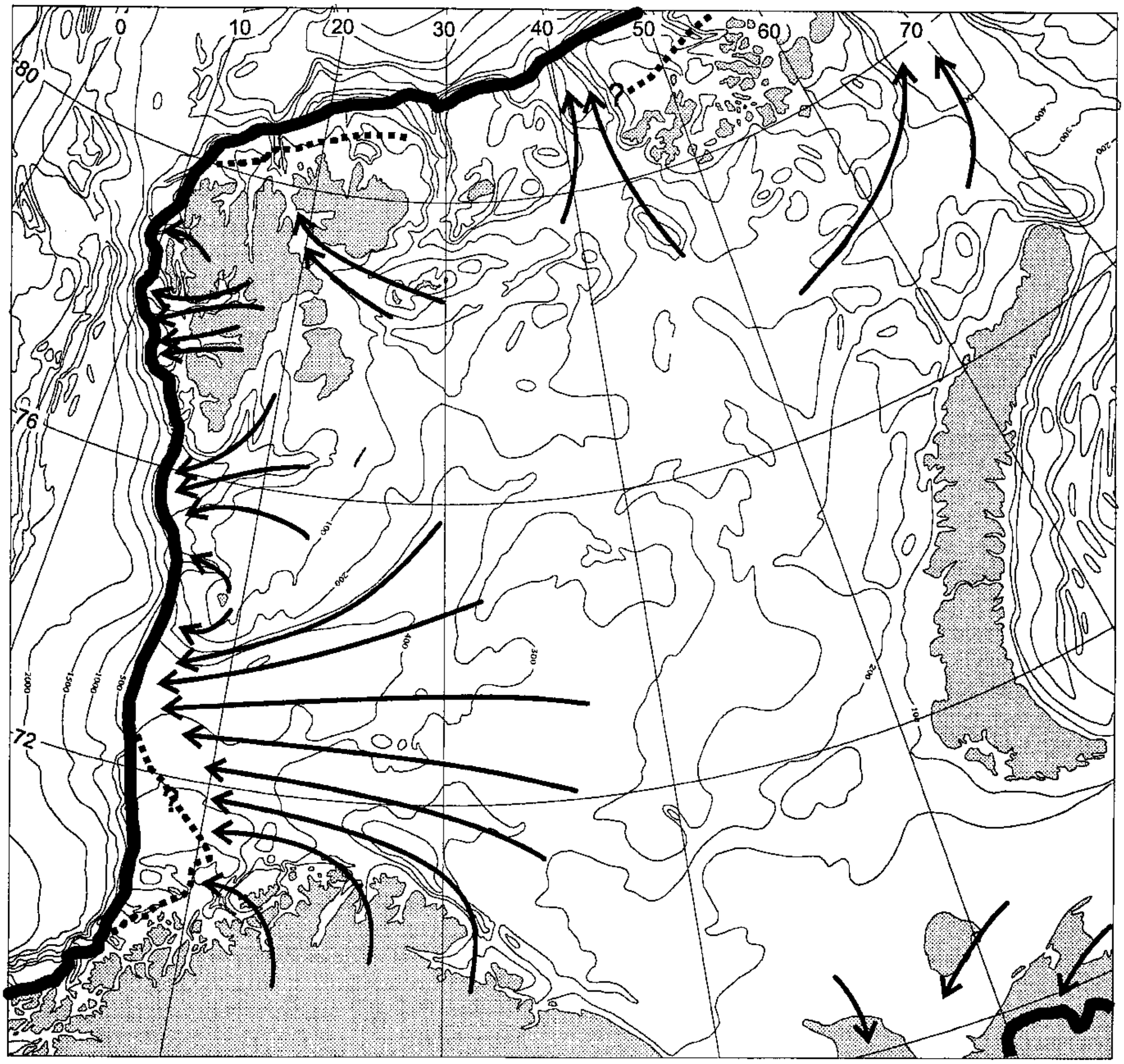

FIG. 12. Reconstruction of the margin of the Late Weichselian Svalbard–Barents ice sheet. The dotted lines show minimum proven extent in some areas. Conceptual flow lines are based on geomorphological evidence. For place names, see Fig. 2.

fjords troughs. The seismic stratigraphy from the shelf between the troughs shows deposition of moraine ridges with extensive erosion on the proximal side (Solheim *et al.*, 1996; Andersen *et al.*, 1996). We find it most likely that the ice sheet also reached the shelf edge in these areas. Such an ice extent cannot be explained convincingly by only a local ice cap located on Svalbard, and implies that a large Barents Sea ice sheet inundated the entire archipelago.

A major question still to be answered concerns the ice margin on the northern shelf of Svalbard and the Barents Sea. In the northwest, the ice margin can be ascribed to the Amsterdamøya–Danskøya area (Fig. 4) that sits close to the shelf break. The moraines in the sound between the islands (Salvigsen, 1977) were probably deposited at or close to the maximum Late Weichselian ice extent. To the north of Svalbard, a minimum extent is shown by the moraine mapped off Raudfjorden (Liestøl, 1972) and in Liefdefjorden (Salvigsen and Österholm, 1982). However, as there is no change in sediment thickness across the moraines we assume that these probably only represent recessional stages as suggested by Andersen (1981).

We conclude that Late Weichselian ice filled the Franz Victoria Trough down to ca 500 m water depth. Further, we assume that the westward continuation of the ice margin also covered the shallow shelf north of Kvitøya and Nordaustlandet (Fig. 12).

Another major uncertainty regarding the ice-sheet margin and ice-sheet topography during the last glacial maximum is the southeastern part of the Barents Sea and adjacent land areas in northern Russia. The

Barents ice sheet was probably contiguous with the Kara Sea ice sheet. The ice that inundated the coastal areas of northern Russia were derived from this confluence zone. During the maximum glaciation, the ice flow into the Pechora lowland was dominated by flow from the Kara Sea.

A consequence of our reconstruction is that practically all land areas in the Barents Sea area were covered by glacier ice during the Late Weichselian. The reconstructed ice drainage pattern from the land areas, e.g. Svalbard and coastal Norway, shows predominantly topographically-controlled ice movements, whereas the large-scale reconstruction implies that ice movements of a much more regional character also occurred. This discrepancy can probably be explained by the overprint in ice movements imposed on the higher relief land areas during the late-glacial and deglaciation phases.

DURATION OF THE LAST GLACIAL MAXIMUM

Until recently, there has been little information on the onset and duration of the Late Weichselian glaciation of the Barents Sea. No stratigraphic successions that contain a continuous development from the last interstadial, through the glaciation and deglaciation phase have been found. However, some estimates can be made about the nature of the western part of the ice sheet based on: (1) amino acid epimerization rates in pre-Late Weichselian molluscs from Spitsbergen; (2) radiocarbon-dated molluscs in tills in Bjørnøyrenna; and (3) sediment cores from the western slope and the deep sea.

The amino acid epimerization rate in mollusc shells is both time- and temperature-dependent (Miller and Brigham-Grette, 1989) and can, thus, be used for time estimates if the temperature is known. In Linnéddalen on the west coast of Svalbard (Fig. 2), a beach terrace 87 m a.s.l. was overridden by the Late Weichselian glacier (Mangerud *et al.*, 1992, 1998). Molluscs in beach sediments underlying a till yielded radiocarbon age estimates of 36 ka, and amino acid ratios of 0.019 ± 0.002. This value overlaps within 1 SD with the mean D/L ratio of $0.016 + 0.003$ obtained from 42 analyses of 10–13-ka-old shells from the west coast. Based on the difference in these ratios, Mangerud *et al.* (1992) calculated the duration of ice cover to have been between 3000 years (warm-based ice) and 10,000 years (cold-based ice). With a local deglaciation of 12.3 ka (Fig. 3) (Mangerud and Svendsen, 1990), the west coast of Svalbard must have remained unglaciated until at least 22 ka. Similar results were obtained from the Kapp Ekholm section (Mangerud and Svendsen, 1992). We assume that the lack of marine sediments and molluscs from the period 40–20 ka on land reflects that sea level was below the present day coast line, as should be expected from global eustasy (Chappell and Shackleton, 1986).

Evidence for Middle and Late Weichselian ice-free conditions has been found in Bjørnøyrenna (Fig. 3). Glaciers flowing out the trough picked up marine molluscs and incorporated them into tills (Hald *et al.*, 1990; Vorren *et al.*, 1990; Elverhøi *et al.*, 1993). Molluscs recovered from glacial sediments in several cores rendered a series of radiocarbon ages ranging from 42 to 21.6 ka (Fig. 3), suggesting that glacier ice first reached the 300–350 m depth contour after 21.6 ka. Radiocarbon ages from the debris flow lobes on the large fans suggest that the glacier reached the shelf edge after 17.5 ka (Laberg and Vorren, 1995) and after 19.6 ka off Isfjorden (Andersen *et al.*, 1996). Thus, the glacier rested at the outer shelf for only 3–5000 years.

The marine-based Barents Sea ice sheet had a strong control on sediment flux to the adjacent deep sea. In addition to clay and silt-sized particles transported in the water column, all grain sizes were carried out by icebergs as ice-rafted detritus (IRD). For the fine-grained particles other modes of transport cannot be ruled out and IRD is, therefore, identified as pertaining to particles > 500 g. Studies of sediment cores from the continental slope off Svalbard (Elverhøi *et al.*, 1995a; Andersen *et al.*, 1996) have provided ages relating to the glacial signal derived from the ice sheet. These events were also correlated directly with the palaeoceanographic regime (Hebbeln *et al.*, 1994). Prior to 23 ka the cores from the slope record an overall low sedimentation rate and a low IRD signal. Elverhøi *et al.* (1995a) concluded that there was no grounded ice in the Barents Sea at this time, and that glaciers on Svalbard were restricted to the fjords. However, some reworked palynomorphs in the sediments may indicate more extensive glaciation over eastern Svalbard and the northern Barents Sea. Ice-free conditions in the southern and central Barents Sea during this time are also supported by the radiocarbon ages from the Bjornoyrenna area which suggest ice-free conditions from ca 30 to 22 ka (Fig. 3). After 23 ka, the cores show a higher sedimentation rate, higher input of organic matter, and the presence of bedrock fragments with a northern and eastern Barents Sea provenance (Elverhøi *et al.*, 1995a). This mode of deposition continued until 19.4 ka, when the overall hemipelagic sedimentation rate was lowered, although there was still a high input of IRD consisting predominantly of Fennoscandian crystalline grains. The onset of ice retreat from the shelf break off Isfjorden occurred at 14.8 ka (see above). The initiation of the ice-sheet retreat at this time is supported by the distinct melt-water spike recorded in the Fram Strait sediments (Jones and Keigwin, 1988), and increased deposition of coarse-grained IRD on the upper slope coinciding with the North Atlantic Heinrich event H1 (Elverhøi *et al.*, 1993).

These data also suggest a relatively short duration for the LGM, where ice advanced onto the western shelf after 22 ka, and culminated at the shelf break between ca 19 and 15 ka before the onset of the last deglaciation.

THE LAST DEGLACIATION

The ice recession from the LGM occurred stepwise, and our reconstruction of the ice distribution at 15 and 12 ka is shown in Fig. 13. Generally, radiocarbon ages from the base of post-glacial marine sediments above till or beach terraces close to the marine limit, yield progressively younger ages from the distal to the more proximal parts of the former ice sheet (Fig. 3), supporting the assumption that the sediments were deposited in front of a retreating glacier.

The onset of deglaciation at around 15 ka is supported by well-dated oxygen isotope records from the continental slope to the west of Spitsbergen which reflect a distinct meltwater event at this time (Elverhøi *et al.*, 1995a). It is assumed that rising sea level affected the marine section of the ice sheet, causing iceberg calving within Bjørnøyrenna (Fig. 13). The sediment succession in the cores from the continental shelf to the west of Spitsbergen indicates that the ice front started to recede at around 14.8 ka (Svendsen *et al.*, 1996) or perhaps as early as 16.4 ka (Cadman, 1996). This agrees with previous results obtained from the confluence area between the Scandinavian and Barents Sea ice sheets off the mainland of northern Norway, where the deglaciation has been estimated to between 16.2 and 13.7 ka (Vorren *et al.*, 1988).

The rate and extent of this early stage of deglaciation after 15 ka is not known well. Investigations of raised marine sediments on land show that the extreme western coast of Spitsbergen was partly ice free by 13 ka or

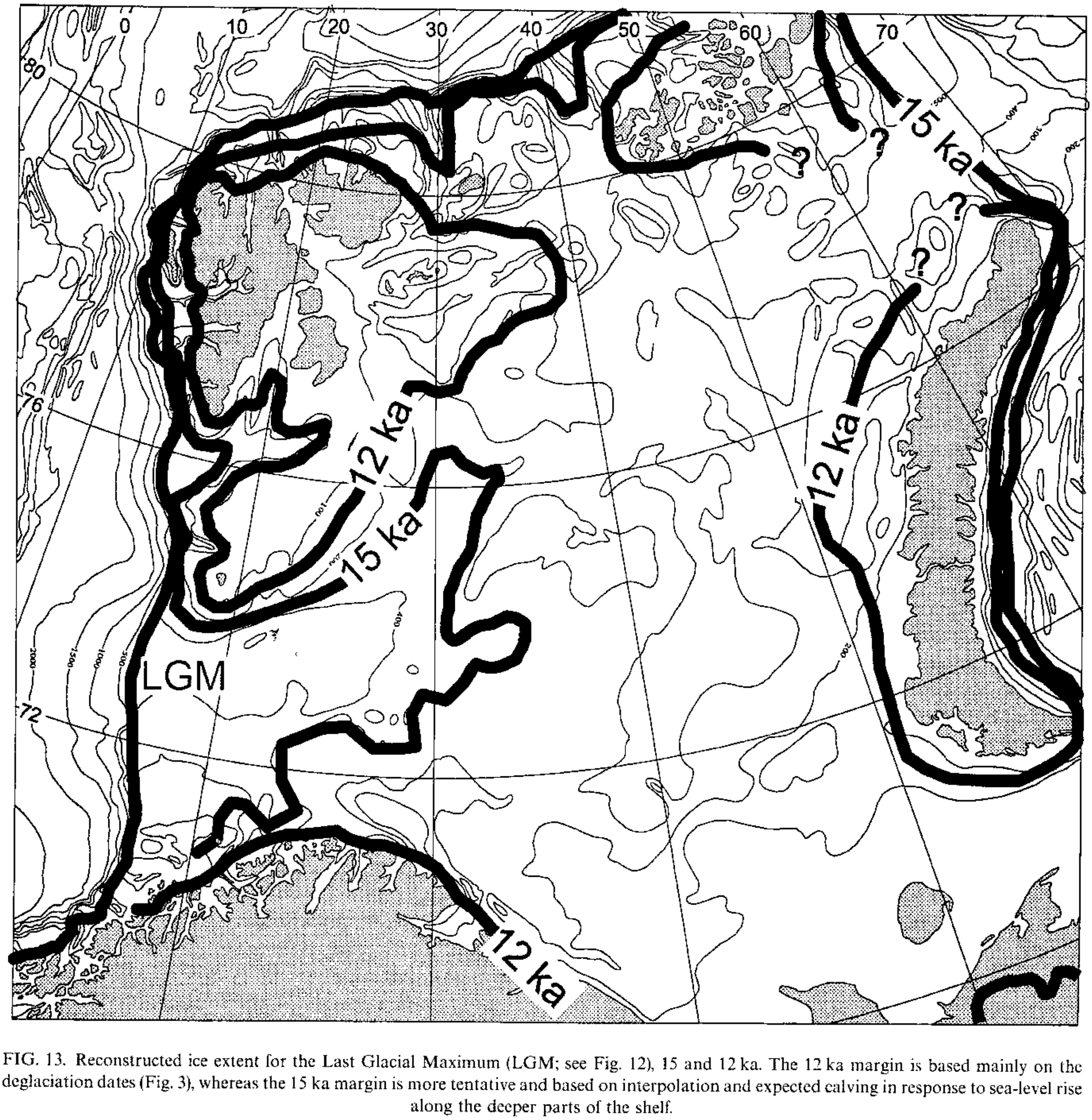

FIG. 13. Reconstructed ice extent for the Last Glacial Maximum (LGM; see Fig. 12), 15 and 12 ka. The 12 ka margin is based mainly on the deglaciation dates (Fig. 3), whereas the 15 ka margin is more tentative and based on interpolation and expected calving in response to sea-level rise along the deeper parts of the shelf.

shortly after (Forman, 1989; Landvik *et al.*, 1992a; Mangerud *et al.*, 1992). Sediment cores from the continental shelf to the southwest of Novaja Zemlya and the inner part of the Franz Victoria Trough (Fig. 3) show that a significant part of the Barents Sea was deglaciated by 12 ka (Fig. 13). This glacial retreat corresponds with a pronounced increase in the flux of glacimarine sediments and is inferred to reflect increased melting due to a sudden climatic warming at this time (Elverhøi *et al.*, 1995a; Svendsen *et al.*, 1996).

Along the western margin of Spitsbergen this second stage of deglaciation was interrupted by a local glacial readvance that culminated on the continental shelf to the west of Isfjorden shortly after 12.4 ka, as indicated by four AMS ages (12.6–12.4 ka) on molluscs in till (Svendsen *et al.*, 1996). This readvance correlates with the terminal moraine in the Kongsfjorden area to the north (Lehman and Forman, 1992) (Fig. 2), and may also correlate with the moraine lobes in front of Woodfjorden, Liefdefjorden, Raudfjorden, Smeerenburgfjorden and in the sound between Amsterdamøya and Danskøya (Fig. 2). This glacial readvance is correlative with a re-advance of the Fennoscandian ice sheet along the west coast of Norway (Andersen, 1968; Anundsen, 1977; Mangerud, 1977; Vorren *et al.*, 1988). Shortly after 12.3 ka the ice front receded inside the mouth of Isfjorden (Mangerud and Svendsen, 1990), and the retreat most likely continued during the Allerød period.

During the Younger Dryas, the inner branches of Isfjorden were occupied by outlet glaciers, probably draining the remnant of the Svalbard–Barents Sea ice sheet (Mangerud *et al.*, 1992; Svendsen *et al.*, 1996). The glacier in Van Mijenfjorden had its terminus close to the fjord mouth (Mangerud *et al.*, 1992). Relative sea level curves from the west coast of Spitsbergen reflect a delayed glacioisostatic uplift during the Younger Dryas that points to a stable or growing ice load in the east (Landvik *et al.*, 1987; Forman, 1990; Mangerud and Svendsen, 1990; Lehman and Forman, 1992). Thus, there is evidence to suggest that the ice recession paused and possibly the fjord glaciers that were connected to the ice sheet advanced during the Younger Dryas, as suggested by Boulton (1979a). In contrast, local glaciers on the west coast of Spitsbergen were even smaller during the Younger Dryas than during the Little Ice Age (Mangerud and Svendsen, 1990). The cause for such a different response is not clear, but possibly the ice sheet received most of the precipitation from the Barents Sea. The eastern part of Svalbard was ice covered until the end of the Younger Dryas (Landvik *et al.*, 1995) (Fig. 3).

Even though the question of a Younger Dryas ice advance has not been resolved, numerous radiocarbon ages from eastern Svalbard and from the inner fjord branches on western Spitsbergen show that the rest of the ice sheet in the northwestern Barents Sea melted rapidly around 10 ka as a result of the sudden climatic warming at the transition to the Holocene. During the early and mid Holocene the glacier cover on Svalbard was greatly reduced (Svendsen and Mangerud, 1992). A regrowth of the glaciers seems to have occurred during the Late Holocene, culminating in maximum ice extent during the Little Ice Age (Elverhøi *et al.*, 1995b; Svendsen and Mangerud, 1997).

NUMERICAL MODELLING OF THE LAST ICE SHEET

Numerical modelling of ice sheets can provide quantitative information regarding the evolution of palaeo-ice masses. However, geological observations are required in order to constrain model results. In this section we will review the use of numerical models to understand the evolution of the Barents Sea ice sheet, its distribution and the palaeoenvironment required for such an ice sheet to form. The glaciation of the Barents Shelf can be modelled in two separate ways: (1) time-dependent isostatic models where the ice loads are determined by matching measurements of raised shorelines to models of lithospheric deformation (Elverhøi *et al.*, 1993; Lambeck, 1995, 1996); and (2) glaciological (ice sheet) modelling (Siegert and Dowdeswell, 1995a,b; Siegert and Fjeldskaar, 1996).

Isostatic models

The isobase map (Fig. 9) shows the crustal deformation and rebound that reflect the redistribution of glacier ice and sea water on the Earth's surface. Recent developments in the geophysical understanding of such isostatic deformation (see Lambeck, 1993) have made it possible to reconstruct past ice sheet distributions from post-glacial relative sea level change.

Barents ice sheet models

Elverhøi *et al.* (1993) applied a non-spherical layered viscoelastic fluid model (Fjeldskaar and Cathles, 1991a,b), coupled with hydro-isostatic calculations, to the Fennoscandian ice sheet in order to determine if the Barents ice sheet had any isostatic significance along the northern coast of Fennoscandia. By using ice margin data from Denton *et al.* (1981) and theoretical ice profiles, this exercise suggested that significant parts of the Barents ice sheet was deglaciated by 15 ka. (Lambeck, 1995, 1996) used a different approach to directly model the Barents ice sheet. He used a glacio-hydro-isostatic rebound model where the Earth's rheology is treated as a three-layer model using parameters from Fennoscandia (Lambeck, 1995). With the input of different ice sheet extents, the model was run to produce relative sea level curves which could be compared to observed curves from the Barents Sea region.

In an initial study (Lambeck, 1995), two different ice sheet distribution scenarios were used as input to the model: (a) a minimum-extent model (Fig. 14a), where ice was restricted to the Barents Sea and the west and northwest coasts of Svalbard, and the entire Kara Sea

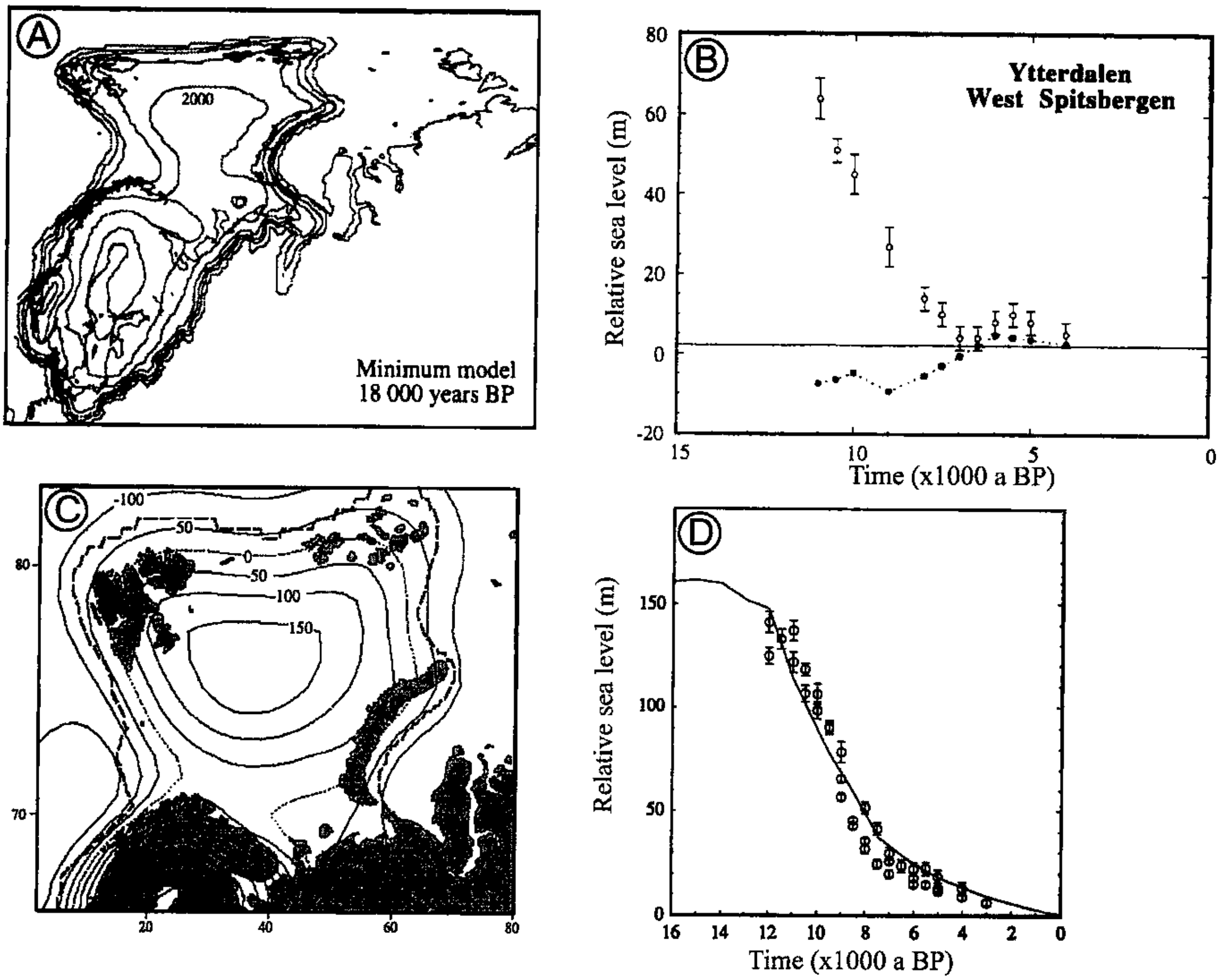

FIG. 14. Different ice sheet models (A and C) have been the input in modelling relative sea-level curves for the southwest coast of Spitsbergen. (A) Ice was restricted to the Barents Sea and the west and northwest coasts of Svalbard, while the entire Kara Sea remained ice free. Ice thickness in metres. Lambeck (1995) showed that this ice sheet could not generate the observed relative sea-level curve (B) from Ytterdalen on the north coast of Bellsund (Fig. 4). (C) Assuming that ice extended to the shelf west of Spitsbergen and the Kara Sea also was glaciated, the modelled curve (D) is in good agreement with the observed relative sea-level change shown by a composite of three different curves from the southwest coast of Spitsbergen (A) and (B) reproduced from Quaternary Science Reviews, 14, 1–16 (1995), Lambeck, K. "Constraints on the Late Weichselian ice sheet over the Barents Sea from observations of raised shorelines.".

remained ice free; and (b) a maximum-extent model (Fig. 14c), where ice extended to the shelf west of Spitsbergen and the Kara Sea was also glaciated.

The minimum-extent model satisfactorily reproduced the relative sea level curves from Franz Josef Land, suggesting that the assumed ice extent to the northern shelf was appropriate (Lambeck, 1996), but that ice retreat was faster than assumed (Lambeck, 1995). For the west coast of Svalbard, the relative sea level predictions from the minimum model, with an ice margin close to the present coast, lie significantly below the observed values (Fig. 14b). As the modelled ice extent is insufficient to reproduce the observed values, the experiment clearly indicates that the ice margin was at the shelf edge west of Svalbard. In the central and northern Barents Sea, however, the maximum-extent model gave an overall better agreement with observed sea level change than did the minimum-extent model.

Based on the results from these two model experiments, Lambeck (1996) proposed a revised model with ice extended to the shelf edge to the west and north, but without substantial ice over the Kara Sea and west Siberia (Fig. 14c). The proposed ice thickness over the Barents Sea was roughly 3400 m. If a substantial ice sheet is kept over Spitsbergen until 13 ka, the model gives a reasonable fit with sea level curves from most of the region, and especially the west coast of Svalbard (Fig. 14d).

A mantle viscosity-dependent model

Based on analyses of the deglaciation of Fennoscandia together with data on the tilt of palaeoshorelines and the present rate of uplift, Fjeldskaar and Cathles (1991a,b) and Fjeldskaar (1994) concluded that the mantle in the area has a viscosity close to 10^{21} Pa s, and is overlain by a 75 km thick asthenosphere with a viscosity of 1.3×10^{19} Pa s. Previous papers also strongly suggested (on the basis of the observed shoreline tilt) that the lithosphere rigidity in Fennoscandia is less than 1014 Nm. It has also been shown (Fjeldskaar, 1994) that the predicted forebulge is in accordance with the observations in offshore areas. Similar modelling is shown here for Svalbard and Bjørnøya.

The isostatic model.

The Earth is modelled by a layered viscous model with an elastic lithosphere of constant thickness. With this flat Earth model, we are able to treat the isostatic problem analytically by the Fourier transform technique. The method used here is described in Cathles (1975) and Fjeldskaar and Cathles (1991a). The elastic lithosphere is treated as a low-pass filter. Loads of small size are thus supported by the lithosphere itself, not by buoyancy. A measure of the strength of the lithosphere is a parameter called the flexural rigidity. The models have been run with a lithosphere rigidity of 2×10^{23} Nm.

When a load is applied on the Earth's surface there is an immediate elastic displacement. When stress is released the initial elastic displacement will be recovered. The method for calculating the elastic response is given in Cathles (1975). For a layered elastic Earth the solution is more complicated, and we use the propagator technique described in Cathles (1975).

Matching the Svalbard relative sea-level curves.

In this study the model was run to reconstruct 12 different observed sea level curves from the Svalbard archipelago (see Fig. 15). The modelling procedure is carried out using two different mantle rheology models. The first model has the same rheology as that which gave the best fit with the observations in Fennoscandia, a 75-km thick asthenosphere of viscosity 1.3×10^{19} Pa s overlying a mantle of viscosity 10^{21} Pa s. The second model uses a uniform mantle viscosity of 10^{21} Pa s.

In contrast to Fennoscandia, the uniform model gives the best fit to the relative sea-level data. The general trend is that the asthenosphere model gives a larger and faster post-glacial uplift. However, the observations show that there has been a slow uplift in the area, indicating a relatively high mantle viscosity, e.g. Agardhbukta (Fig. 15). For locations as far north as Nordaustlandet, the observed uplift also follows a slow trend. The uniform model is most easily fitted to such a trend, and the misfit with the observations can probably be explained by a delayed deglaciation of the northernmost parts of the archipelago.

For the westernmost location (e.g. Bellsund and Erdimannflya; Fig. 15), both models produce too little uplift. One reason for this apparent lack of uplift is that the area was glaciated further to the west than indicated in the models. Variations in lithosphere rigidity cannot increase the fit of any models, because an increased flexural rigidity would tend to increase the rate of uplift.

Bjørnøya.

There are no observed post-glacial shorelines on Bjørnøya (Salvigsen and Slettemark, 1995). The theoretical sea-level curve (Fig. 15) is in accordance with the lack of observed shore lines, and the post-glacial relative sea level has never been above present sea level. The model shows that the island experienced subsidence since late-glacial times. A present subsidence rate on the island of 3 mm/year is predicted by the asthenosphere model, whereas 5 mm/year is predicted by the uniform model.

Mantle viscosity.

On the basis of the modelling of post-glacial shoreline displacement on Svalbard it is suggested that the viscosity structure in the area is different from the one in Fennoscandia. A model with uniform mantle viscosity gives a better fit to the observed slow uplift in the area than the model with Fennoscandian rheology (low viscosity asthenosphere).

Glaciological modelling

Previous models of the Svalbard–Barents Sea ice sheet

Previous ice sheet modelling of the Barents Ice Sheet (Hughes, 1979) was performed using estimated ice flow lines, with the ice-sheet terminus located at geologically-inferred margins. By running the models with constant climate conditions until stability was reached, steady-state ice-sheet profiles were obtained for each flow line (Denton *et al.*, 1979; Fastook *et al.*, 1979; Hughes, 1979, 1981; Denton and Hughes, 1981). The Barents ice sheet was modelled as a component of a larger Eurasian ice sheet, and a maximum ice thickness of 2.1 km was obtained over Novaya Zemlya. A model where also the basal sliding and sediment was taken into account was presented by Lindstrom (1990). Isaksson (1992) used a similar modelling approach, and obtained a 1.7 km high dome east of Edgeøya by treating the Svalbard and Barents Sea area separately from the Eurasian ice sheet.

Denton and Hughes (1981) and Hughes (1987) predicted that the initiation of the Svalbard–Barents Sea ice sheet could be achieved only after permanent sea ice had thickened to form an ice shelf and subsequently grounded over the sea floor. However, the likelihood of the emplacement of an ice shelf over the deeper parts of the Barents Sea has been questioned, since the underlying water convection (and hence the basal melting of the ice shelf) was not accounted for (e.g. Elverhøi *et al.*, 1993).

Peltier (1988) predicted the Earth's residual rotational signature that was caused by the decay of the last ice sheets, and found that a large ice sheet over the Barents Sea during the Late Weichselian is required.

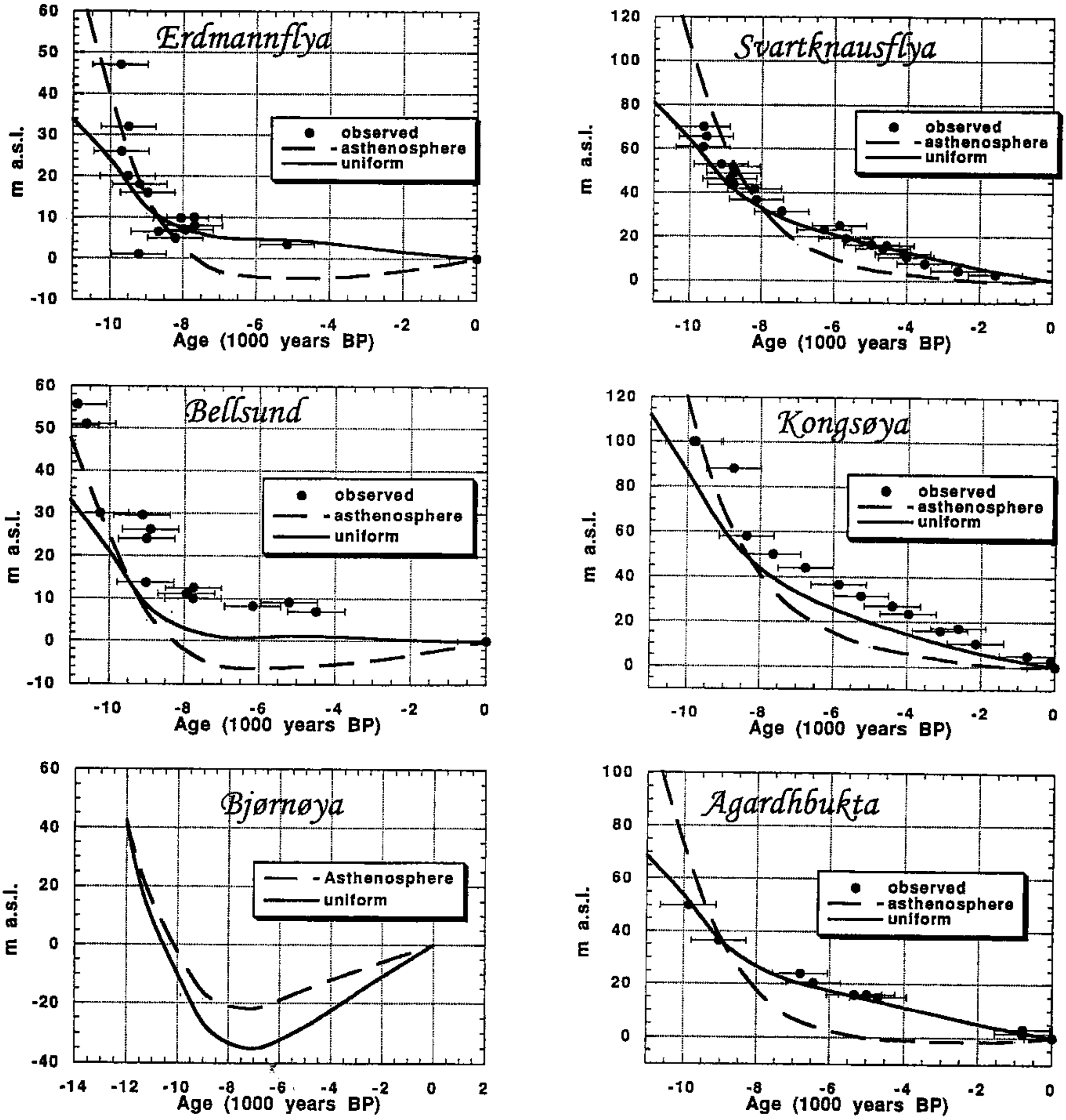

FIG. 15. Observed vs theoretical shoreline displacement curves for two different earth models: (a) with a low viscosity asthenosphere (stippled lines); and (b) a uniform mantle (solid lines). The observations are from the following sources: Erdmannflya (Salvigsen *et al.*, 1990); Svartknausfdya (Salvigsen, 1979); Bellsund (Landvik *et al.*, 1987); Agardhbukta (Salvigsen and Mangerud, 1991); and Kongsøya (Salvigsen, 1981).

A global isostatic model of the Earth's response to the surface unloading during deglaciation was designed to examine the possible distribution of ice masses at the LGM, and to discover how they decayed during deglaciation Tushingham and Peltier, 1991; Tushingham and Peltier, 1993). The LGM ice sheet distribution that was produced by this method comprised a grounded, 2.2-km thick ice sheet over the Barents Sea at the LGM, with ice margins similar to those predicted by Denton *et al.* (1981).

Modelling strategy

Our modelling strategy represents an inverse approach, where model results are forced to match with geological information. The ice sheet model was run initially with what were considered the most likely environmental boundary conditions for the Late Weichselian. Results from this exercise were then compared with geological information on ice sheet size and extent, and the timing/rate of ice sheet decay. Two

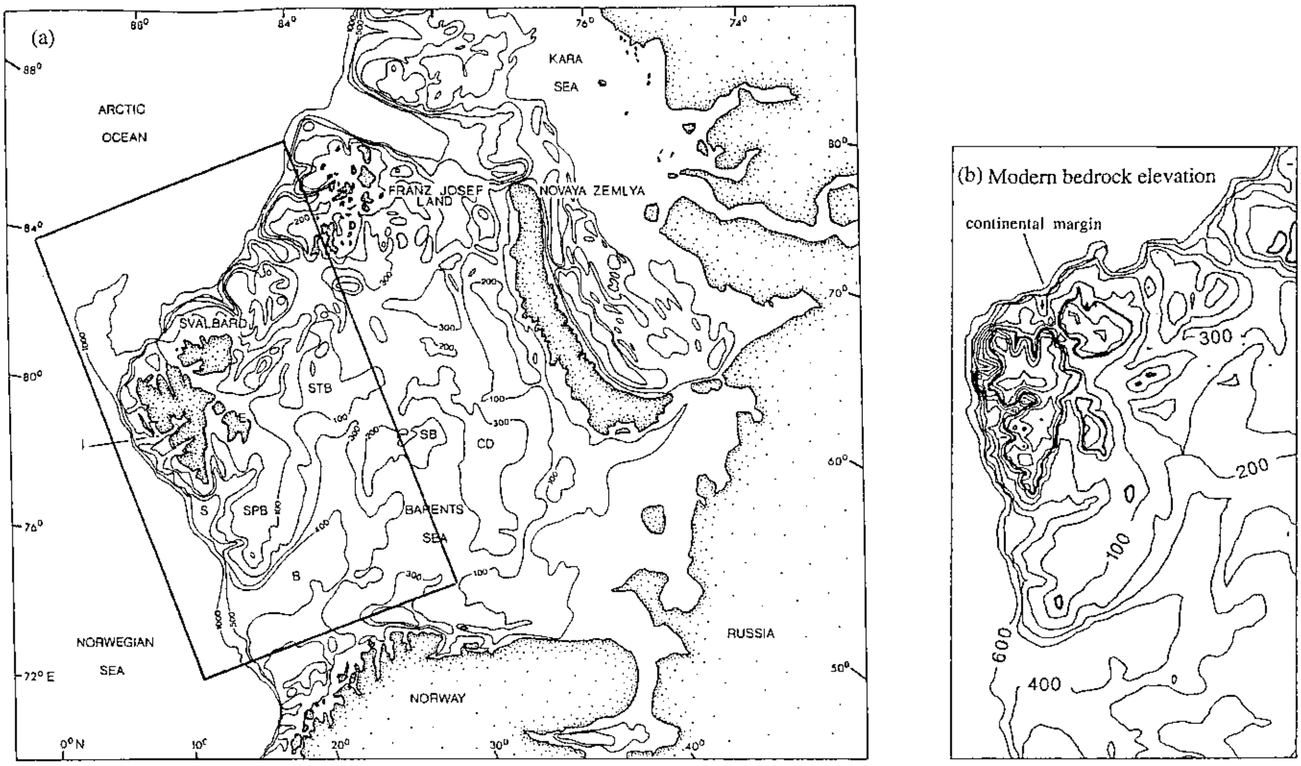

FIG. 16. (a) The location and bathymetry of the Barents Sea. E, Edgeøya; B, Bjørnøyrenna; S, Storfjordrenna; I, Isfjorden; SB, Sentralbanken; STB, Storbanken; SPB, Spitsbergenbanken; CD, Central Deep. The frame around the western Barents Sea denotes the position of the model boundary. (b) Modern topography and bathymetry of the Svalbard–Barents Sea region, used as bedrock input to the model.

strategies were developed in order to explain any apparent mismatch between field and model data. First, an ice sheet sensitivity experiment was performed by varying the model inputs until the calculated ice sheet was compatible with the geological data. Secondly, the ice sheet model was coupled with results obtained from isostatic models as discussed above (Siegert and Fjeldskaar, 1996).

The ice-sheet model

The ice sheet model is based on the continuity equation for ice (Mahaffy, 1976), and is discussed in more detail by Siegert and Dowdeswell (1995a). The time-dependent change in ice thickness is associated with the specific net mass budget of an ice cell, and ice temperature is calculated from the steady-state method of Robin (1955). However, this solution does not account for horizontal heat advection and is only applicable close to the ice divide. Far from the modelled ice divide, the mean ice temperature of a cell is not allowed to exceed $-5°C$, a temperature often used in isothermal models to determine the flow law parameter (Payne *et al.*, 1989). Grounded ice velocity is calculated as the sum of depth-averaged ice deformation (Paterson, 1994) and basal sliding (Budd *et al.*, 1984). The basal sliding velocity is related to the effective pressure. Bedrock elevation change, caused by variations in ice thickness, is determined by an asthenospheric diffusion equation (Oerlemans and van der Veen, 1984).

Time-dependent modelling was performed in calendar years (cal year), and radiocarbon ages (indicated by ka) derived from the geological record are converted to calendar years using the calibration curve of Stuiver and Reimer (1993).

Model boundary conditions

Based on erosion-rate estimates from Svalbard (Svendsen *et al.*, 1989; Elverhøi *et al.*, 1995b), it is assumed that at 30,000 years ago, the bedrock elevation of the Svalbard–Barents Sea region on a large scale was similar to that of today. The bedrock elevation array is composed of 2800 (70 north by 40 east) cells, with a width of 20 km per cell, and was calculated from topographic maps and radio-echo sounding data on modem ice thickness (Dowdeswell *et al.*, 1986) (Fig. 16).

Local sea level was severely affected by the gravitational attraction of large nearby ice masses (e.g. Clark *et al.*, 1978; Fjeldskaar and Kanestrøm, 1980). To account empirically for this glaci-gravitational effect, sea level within the Barents Sea is lowered at 75% of the eustatic level during glaciation (Chappell and Shackleton, 1986). In ice-sheet sensitivity experiments (discussed below), relatively large changes in sea-level depression ($\pm 25\%$) did not adversely alter the model results presented here (Siegert and Dowdeswell, 1995b).

Iceberg calving was calculated by a depth-related calving function deduced from a statistical analysis of calving glaciers from several polar locations, including Svalbard (Pelto and Warren, 1991).

Environmental forcing

The model requires climatic inputs in the form of air temperature and precipitation and their behaviour with respect to altitude. There are several lines of evidence indicating that precipitation conditions similar to the present Polar Mix (PX) (Pelto *et al.*, 1990) existed over the Barents Sea during three episodes within the Late Weichselian. Hebbeln *et al.* (1994) interpreted sea-ice free conditions in the eastern Norwegian–Greenland Sea both between 27–18, and 17–15 ka were interpreted from sedimentological and foraminiferal assemblage data. Additionally, after 14 ka, diatom records from sea-floor sediment cores indicate that ice-free conditions remained on the eastern side of the Norwegian–Greenland Sea into the Holocene (Koç *et al.*, 1993). In the remaining periods, due to the likely absence of a local moisture source, a Polar Continental (PC) accumulation function (Pelto *et al.*, 1990) is used. We assume that accumulation on the ice sheet decreased towards the east due to the increasing distance from the primary moisture source (Siegert and Dowdeswell, 1995a).

The model relates the equilibrium line altitude (ELA) to temperature through an adiabatic lapse rate of 5.1°C/km (Fortuin and Oerlemans, 1990), and the air temperature depression over the Barents Sea at the glacial maximum is put at 10°C (Manabe and Bryan, 1985). An assumption is made that, since glaciers on Svalbard were not significantly larger at 30 ka than today (Mangerud *et al.*, 1992, 1998), the environmental and mass balance conditions at 30 and 10 ka were similar to those of today. Air temperature through time has been calculated using a carbon dioxide forcing function based on high latitude ice-core records (Siegert and Dowdeswell, 1995a).

Minimum model of glaciation

An ice sheet evolution model for a minimum reconstruction was presented by Siegert and Dowdeswell (1995a) (Fig. 17). After initiation about 28,000 cal years ago, the ice sheet had grown to its maximum size at 20,000 cal years ago, and at this time occupied only the northwestern Barents Sea (Fig. 17b). They also showed that the surface elevation of this ice-sheet model was controlled by the underlying bedrock elevation as shown in Fig. 16b.

Sensitivity experiments (Siegert and Dowdeswell, 1995b) suggested that the modelled ice sheet is relatively stable with regard to changes in inputs controlling the mass balance. Even relatively large ($\pm$ 25%) changes in the inputs of accumulation, iceberg calving and sea level did not adversely affect the main conclusions and results of the model. Significant changes ($\pm$ 10%) in the dynamics of the ice sheet produced small ice volume variations.

Comparison with the geological observations

The last glacial maximum

No grounded ice was predicted to have existed within Bjørnøyrenna at 20,000 cal years ago (Fig. 17). Therefore, the model results are in disagreement with geological evidence from the Bjørnøya fan (Laberg and Vorren, 1996; Vorren and Laberg, 1996).

The last deglaciation

Time-dependent model output of ice volume, surface area and rates of ice accumulation and iceberg calving for the minimum-extent reconstruction (Fig. 16g,h) indicate the evolution of the ice sheet through the period of deglaciation. Although the model's timing of the onset of deglaciation (Fig. 17g) correlates well with the age of the light oxygen isotope peak at 14.8 ka (i.e. at about 16,500 cal year), the predicted volume of ice that is lost at 16,500 cal yr ago is relatively small and cannot alone account for the major melt-water spike.

It was found that if the rate of iceberg calving was left unchanged throughout the model run, then only a relatively small calving peak was produced at 16,500 cal years ago, and too much ice remained at 10,000 cal years ago to account for the observed uplift pattern. When the modelled ELA is below sea level, net surface accumulation would occur on all regions of the ice sheet. At such times, the possible decay of the Svalbard–Barents Sea ice sheet would be determined only by the rate of iceberg calving. The onset of ice sheet disintegration can be pinned at the age of the Fram Strait light oxygen isotope spike at 14.8 ka (i.e. at approximately 16,500 cal years ago). Therefore, the rate of iceberg calving was adjusted by a factor of 2 in a number of model runs to observe how the ice sheet may have responded to rapidly increased rates of calving. The timing of this calving increase was put at 16,500 cal years ago. The ice sheet responded by producing both a melt-water peak compatible with the Fram Strait oxygen isotope record, and a pattern of isostatic uplift similar both spatially and temporally to that reconstructed by Forman (1990) and in this paper (Fig. 9). Although it is difficult to generate the sudden increase in iceberg calving internally within the model, its forced inclusion is necessary to enable the ice sheet to disintegrate in accordance with the local isostatic record (Siegert and Dowdeswell, 1995b).

Modelled properties of the geologically documented glaciation

In this study, the ice sheet from the reconstruction of Siegert and Dowdeswell (1995a) was subjected to further sensitivity experiments to determine which

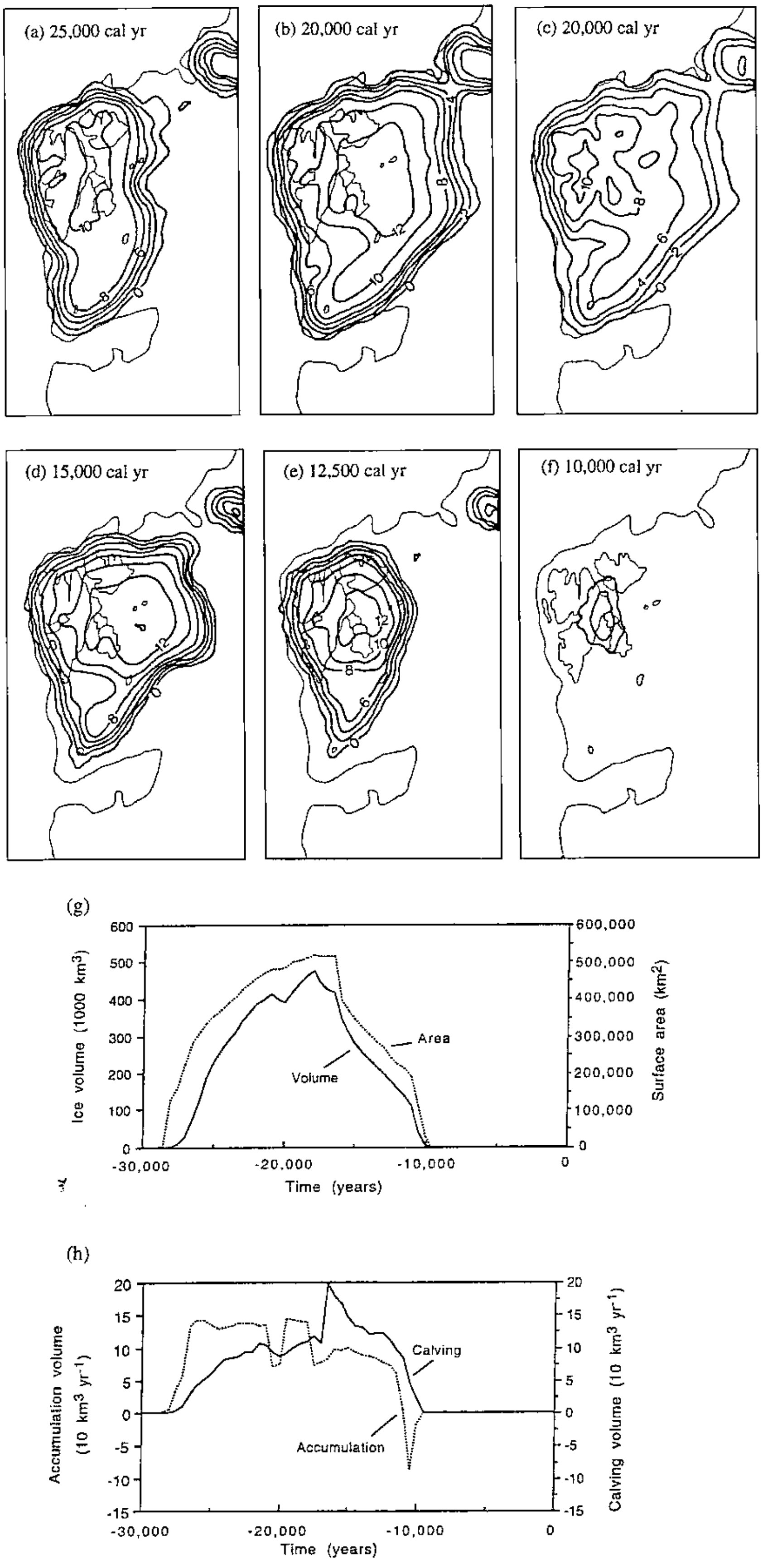

FIG. 17. Minimum reconstruction of the Barents Sea ice sheet from Siegert and Dowdeswell (1995a). Surface elevation contours are in 200 m intervals. (a) Ice thickness at 25,000 cal years. (b) Ice thickness at 20,000 cal years. (c). Ice surface elevation at 20,000 cal years. (d) Ice thickness at 15,000 cal years. (e) Ice thickness at 12,500 cal years. (f) Ice thickness at 10,000 cal years. (g) Ice volume and ice sheet surface area through time. (h). Volumes of iceberg calving and ice accumulation through time in calendar years.

conditions led to the formation of grounded ice within Bjørnøyrenna.

Siegert and Fjeldskaar (1996) proposed modifications of the glaciological model by introducing the effect of crustal forebulge deformation beneath the shallow Barents Sea. By limiting the ice distribution to Svalbard and the surrounding shallow sea, Novaya Zemlya and Fennoscandia, they calculated a forebulge with an amplitude of > 50 m in the central Barents Sea. The forebulge was incorporated into the ice-sheet model's topographic input. Grounded ice was calculated beyond the margin of the ice sheet illustrated in Fig. 17b, when isostatic uplift of 60 m over Sentralbanken occurred. If isostatic uplift in excess of 60 m was modelled, over 500 m of grounded ice formed on Sentralbanken after 5000 year of model time.

If the forebulge exceeds 65 m, Sentralbanken becomes sub-aerially exposed. Grounded ice will form directly over Sentralbanken and connect to ice in the northwestern Barents Sea, resulting in ice volumes up to 40% larger than when 60 m of uplift were modelled. If this ice also was connected to ice masses over Fennoscandia and the Kara Sea, Bjørnøyrenna may have become surrounded by grounded ice. The surface gradient of the ice sheet would, presumably, be controlled by the underlying topography of the region and slope towards Bjørnøyrenna.

The model was able to calculate total grounded ice coverage of the Barents Sea when the rate of iceberg calving was reduced to at least 90% of what was predicted in the standard model based on the depth-related calving function by Pelto *et al.* (1990).

Moreover, the formation of a type of ice sheet shown in Fig. 12 was also possible when greater than 15,000 cal years of model time was available, under constant full-glacial environmental conditions (Fig. 18a,b). However, this situation is in conflict with

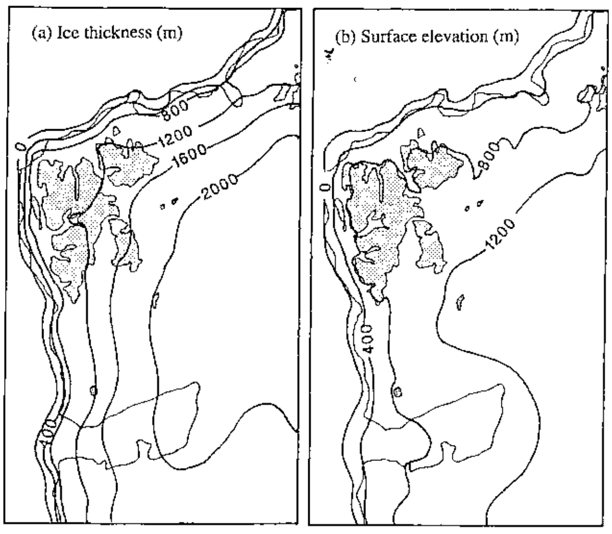

FIG. 18. Results from glaciological modelling experiments of the maximum ice sheet reconstruction. (a) Ice thickness. (b) Surface elevation.

geological evidence showing influx of Atlantic waters also during this time interval (Hebbeln *et al.*, 1994).

DISCUSSION AND SYNTHESIS

The ice-sheet reconstruction we present in this paper (Fig. 12) can be regarded as an end member of a continuous series of successively more extensive glaciation models. It has developed from an original assumption of a more or less non-glaciated Barents Sea and represents a conservative approach, wherein the ice margin has been moved outwards as a result of an increasing amount of field observations.

Some uncertainty still exists with regard to the ice extent in three areas (Fig. 12). (1) Was the northern part of the Barents shelf facing the Arctic Ocean glaciated during the Late Weichselian? Ice has certainly covered the land areas of Svalbard and Franz Josef Land, but it has still not been shown to have extended to the shelf break to the north. However, investigations are underway on this rather inaccessible shelf and preliminary results suggest large similarities with the stratigraphic and morphologic structure of the western Barents margin. (2) In the western border zone of the Fennoscandian and the Barents Sea ice sheets, radiocarbon dating has not proven that the ice extended beyond the moraines mapped by Vorren and Kristoffersen (1986). However, large-scale glaciotectonic features and a limited sediment cover strongly suggest that ice extended to the shelf break in this area during the Late Weichselian. (3) In northern Russia, it has still not been solved whether the ice sheet advanced to the Markhida moraines during the Late Weichselian or if this ice extent is of an older age.

The ice extent to the continental shelf break as suggested by the geological observations has also been supported by isostatic modelling, showing the distribution of ice loading as predicted from the available relative sea-level curves around the Barents Sea (Lambeck, 1995, 1996). In order to produce the observed relative sea level curves, the model required that the ice sheet fill the entire Barents Sea out to the shelf break to the west and to the north (Lambeck, 1996).

The glaciologic modelling suggests that the centre of the ice sheet was situated southeast of Kongsøya. This is compatible with the centre of maximum isostatic uplift (Fig. 9), and the model of Lambeck (1995, 1996) modelling of the maximum ice thickness based on the available relative sea-level curves from the surrounding islands. The pattern of ice movement indicators such as glacial striae, glaciotectonic structures and sub-glacial flutes that can be mapped over eastern Svalbard and the adjacent Barents Sea (Salvigsen *et al.*, 1995) also suggests ice movement from a centre in that region.

The question regarding the thickness of the ice sheet has not been completely resolved. As there are no islands in the area of ice-sheet culmination, the reconstruction of ice-sheet thickness has to be based on calculations from indirect evidence. To fit the relative sea-level curves from Svalbard, Franz Josef Land and Novaja Zemlya, Lambeck (1995) found that the required glacial maximum ice sheet must have been > 800 m thick over western Svalbard and at least 3000 m thick (Lambeck, 1996) over the central Barents Sea. He also proposed that the ice-sheet surface sloped towards Novaja Zemlya and that a smaller ice sheet existed over the Kara Sea. The suggested maximum ice thickness is in excess of the 2000 m proposed from our glaciological modelling. An important prerequisite for the glaciologically modelled ice sheet to attain such a thickness is a very low calving rate. However, considering the alternative of a restricted ice sheet over the central Barents Sea, both models are in agreement regarding the reconstruction of a > 2 km thick ice sheet during the maximum glaciation.

CONCLUSIONS

1. The Late Weichselian ice sheet covered the entire Barents Sea and Svalbard with its adjacent margins.
2. The peak glaciation was relatively short, and the deep troughs on the western Barents shelf were glaciated for only a few thousand years.
3. Numerical modelling of the ice sheet suggests that the build-up was possible due to a very low calving rate, and that a maximum thickness of > 2000 m was attained southeast of Kongsøya.
4. The Barents Sea and Svalbard shelves were largely deglaciated by 12 ka, whereas glaciers remained on the islands of the Svalbard and Franz Josef Land archipelagos until 10 ka.

ACKNOWLEDGEMENTS

This paper is a result of years of stimulating cooperation within the European Science Foundation project "PONAM" (Late Cenozoic Evolution of the North Atlantic Margins). The paper has benefited from numerous discussions with colleagues during these years. Reviews by Julie Brigham-Grette and Peter U. Clark helped to improve the final version. A large portion of the paper was written during the first author's sabbatical year at the Institute of Arctic and Alpine Research, University of Colorado.

REFERENCES

Alm, T. (1993) Øvre Ærasvatn-palynostratigraphy of a 22 000 to 10 000 BP Lacustrine record on Andøya northern Norway. *Boreas* **22**, 171–188.

Andersen, B.G. (1968) Glacial geology of western Troms north Norway. *Norges geologiske undersøkelse* **256**, 1–160.

Andersen, B.G. (1981) Late Weichselian ice sheets in Eurasia and Greenland. *In*: Denton, G.H. and Hughes, T.L. (eds), *The Last Great Ice Sheets*, pp. 1–65. John Wiley & Sons, New York.

Andersen, E.S., Dokken, T.M., Elverhøi, A., Solheim, A. and Fossen, I. (1996) Late Quaternary sedimentation and glacial history of the western Svalbard continental margin. *Marine Geology* **133**, 123–156.

Anundsen, K. (1977) Radiocarbon datings and glacial striae from the inner part of Boknfjord area south Norway. *Norsk geografisk Tidsskrift* **31**, 41–54.

Arslanov, K.A., Lavrov, A.S., Potapenko, L.M., Tertychnaya, T.V. and Chernov, S.B. (1987) *New Data on Geochronology and Paleogeography of the Late Pleistocene and Early Holocene of the Northern Pechora Lowland*. NAUKA, Moscow (in Russian, internal translation to English at University of Bergen, Department of Geology).

Astakhov, V. (1994) *The last glaciation in Russia's European Arctic*. SMR-Report, 13/94, University of Bergen.

Astakhov, V.I. (1979) New data on the latest activity of Kara shelf glaciers in West Siberia. JUGS Project 73-1-24 Prague. *Quaternary Glaciations in the Northern Hemisphere* **5**, 2231.

Bondevik, S., Mangerud, J., Ronnert, L. and Salvigsen, O. (1995) Postglacial sea-level history of Edgeøya and Barentsøya, eastern Svalbard. *Polar Research* **14**, 153–180.

Boulton, G.S. (1979a) Glacial history of the Spitsbergen archipelago and the problem of a Barents Shelf ice sheet. *Boreas* **8**, 31–57.

Boulton, G.S. (1979b) A model of Weichselian glacier variation in the North Atlantic region. *Boreas* **8**, 373–395.

Boulton, G.S., Baldwin, C.T., Peacock, J.D., McCabe, A.M., Miller, G., Jarvis, I., Horsefield, B., Worseley, P., Eyles, N., Chroston, P.N., Day, T.E., and Gibbard, P. (1982) A glacioisostatic facies model and amino acid stratigraphy for late Quaternary events in Spitsbergen and the Arctic. *Nature* **298**, 437–441.

Breuer, D. and Wolf, D. (1995) Deglacial land emergence and lateral upper-mantle heterogeneity in the Svalbard Archipelago—I. First results for simple load models. *Geophysical Journal International* **121**, 775–788.

Budd, W.F., Jenssen, D. and Smith, I.N. (1984) A three-dimensional time-dependent model of the west Antarctic ice sheet. *Annals of Glaciology* **5**, 29–36.

Cadman, V. (1996) *Glacimarine sedimentation and environments during the Late Weichselian and Holocene in the Bellsund Trough and Van Keulenfjorden*, Svalbard. Unpublished thesis, University of Cambridge.

Cathles, L.M. (1975) *The Viscosisty of the Earth's Mantle*. Princeton University Press, Princeton, N.J.

Chappell, J. and Shackleton, N.J. (1986) Oxygen isotopes and sea level. *Nature* **324**, 137–140.

Clark, J.A., Farrel, W.E. and Peltier, W.R. (1978) Global changes in sea level: a numerical calculation. *Quaternary Research* **9**, 265–287.

de Geer, G. (1900) Om Östra Spetsbergens glaciation under istiden. *Geologiska Föreningens Förhandlinger* **22**, 427–436.

Denton, G.H. and Hughes, T.J. (1981) The Arctic Ice Sheet: an outrageous hypothesis. *In*: The last Great Ice Sheets, eds G. H. Denton and T.J. Hughes, pp. 437–467. John Wiley and Sons, New York.

Denton, G.H., Hughes, T.J., Andersen, B.G., Schilling, D.H., Fastook, J.L. and Lingle, C.S. (1981) The last great ice sheets: a global view. In: Denton, G.H. and Hughes, T.J. (eds), *The Last Great Ice Sheets*, pp. 263–317. John Wiley and Sons, New York.

Denton, G.H., Hughes, T.L, Fastook, L.L., Schilling, D.H. and Lingle, C.S. (1979) Reconstruction and disintegration of ice sheets for the CLIMAP 18 000 and 125 000 years experiments: results. *Journal of Glaciology* **24**, 495–496.

Dowdeswell, J.A., Drewry, D.J., Cooper, A.P.R., Gorman, M.R., Liestøl, O. and Orheim, O. (1986) Digital mapping of the Nordaustlandet ice caps from airborne geophysical investigations. *Annals of Glaciology* **8**, 51–58.

Elverhøi, A. and Solheim, A. (1983a) Physical environment western Barents Sea, 1:1,500,000 surface sediment distribution. *Norsk Polarinstitutt Skrifter* **179A**, 1–23.

Elverhøi, A. and Solheim, A. (1983b) The Barents Sea ice sheet—a sedimentological discussion. *Polar Research* **1**, 23–42.

Elverhøi, A., Nyland-Berg, M., Russwurm, L. and Solheim, A. (1990) Late Weichselian ice recession in the central Barents Sea. *In*: Bleil, U. and Thiede, J. (eds), *Geological History of the Polar Oceans: Arctic versus Antarctic*, pp. 289–307. Kluwer, Dordrecht.

Elverhøi, A., Fjeldskaar, W., Solheim, A., Nyland Berg, M. and Russwurm, L. (1993) The Barents Sea ice sheet –a model of its growth and decay during the last ice maximum. *Quaternary Science Reviews* **12**, 863–873.

Elverhøi, A., Andersen, E.S., Dokken, T., Hebbeln, D., Spielhagen, R., Svendsen, J.I., Sørflaten, M., Romes, A., Hald, M. and Forsberg, C.F. (1995a) The growth and decay of the Late Weichselian ice sheet in western Svalbard and adjacent areas based on provenance studies of marine sediments. *Quaternary Research* **44**, 303–316.

Elverhøi, A., Svendsen, J.I., Solheim, A., Andersen, E.S., Milliman, J., Mangerud, J. and Hooke, R.L. (1995b) Late Quaternary sediment yield from the high Arctic Svalbard area. *Journal of Geology* **103**, 1–17.

Elverhøi, A., Hooke, R.L. and Solheim, A. (1998) Land–sea sediment transfer and rates. *Quaternary Science Reviews* (in press).

Emery, K.O. and Aubrey, D.G. (1991) *Sea Levels, Land Levels and Tide Gauges*. Springer-Verlag, New York.

Epshtein, O.G. and Gataullin, V.N. (1993) Lithology and conditions of formation of Quaternary deposits in the eastern part of the Barents Sea (Novaya Zemlya side) *Lithology and Mineral Resources* **28**, 84–94.

Fastook, J.L., Sweet, R. and Hughes, T.L. (1979) A closer look at the proposed Late-Wisconsin–Weichselian Arctic ice sheet. *Journal of Glaciology* **24**, 497–500.

Fjeldskaar, W. (1994) The amplitude and decay of the glacial forebulge in Fennoscandia. *Norsk Geologisk Tidsskrift* **74**, 2–8.

Fjeldskaar, W. and Kanestrøm, R. (1980) Younger Dryas geoid deformation caused by deglaciation in Fennoscandia. *In*: Mörner, N.A., ed. *Earth Rheology and Eustasy*, pp. 569–574. John Wiley & Sons, New York.

Fjeldskaar, W. and Cathles, L.M. (1991a) Rheology of mantle and lithosphere inferred from post-glacial uplift in Fennoscandia. *In*: Sabadini, R., Lambeck, K. and Boschi, E. (eds), *Glacial Isostasy, Sea Level and Mantle Rheology*, pp. 1–19. Kluwer Academic Publishers, Dordrecht.

Fjeldskaar, W. and Cathles, L.M. (1991b) The present rate of uplift of Fennoscandia implies a low-viscosity asthenosphere. *Terra Nova* **3**, 393–400.

Forman, S.L. (1989) Late Weichselian glaciation and deglaciation of the Forlandsundet area, western Spitsbergen Svalbard. *Boreas* **18**, 51–60.

Forman, S.L. (1990) Post-glacial relative sea-level history of northwestern Spitsbergen Svalbard. *Geological Society of America Bulletin* **102**, 1580–1590.

Forman, S.L. and Miller, G.H. (1984) Time dependent soil morphologies and pedogenic processes on raised beaches Bröggerhalvøya, Svalbard archipelago. *Arctic and Alpine Research* **16**, 381–394.

Forman, S.L., Mann, D. and Miller, G.H. (1987) Late Weichselian and Holocene relative sea-level history of Bröggerhalvöya Spitsbergen. *Quaternary Research* **27**, 41–50.

Forman, S.L., Lubinski, D., Miller, G.H., Snyder, J., Matishov, G.G., Korsun, S. and Myslivets, V. (1995) Postglacial emergence and distribution of late Weichselian ice-sheet loads in the northern Barents and Kara Seas Russia. *Geology* **23**, 113–116.

Forman, S.L., Lubinski, D., Miller, G.H., Matishov, G.G., Korsun, S., Snyder, J., Herlihy, R., Weihe, R. and Myslivets, V. (1996) Postglacial emergence of western Franz Josef Land, Russia, and retreat of the Barents Sea ice sheet. *Journal of Quaternary Science* **15**, 77–90.

Fortuin, J.P.F. and Oerlemans, J. (1990) Parameterization of the annual surface temperature and mass balance of Antarctica. *Annals of Glaciology* **14**, 78–84.

Gataullin, V., Polyak, L., Epstein, O. and Romanyuk, B. (1993) Glaciogenic deposits of the Central Deep: a key to the Late Quaternary evolution of the eastern Barents Sea. Boreas **22**, 47–58.

Glazovskiy, A. and Näslund, J-O. (1992) Deglaciation and shoreline displacement on Alexandra Land, Franz Josef Land. *Geografiska Annaler* **74A**, 283–293.

Grosswald, M.G. (1980) Late Weichselian ice sheets of northern Eurasia. *Quaternary Research* **13**, 1–32.

Grosswald, M.G. (1993) Extent and melting history of the Late Weichselian ice sheet, the Barents–Kara continental margin. In: Peltier, W.R. (ed.), *Ice in the Climate System, NATO ASI Series*, pp. 1–20. Springer-Verlag, Berlin.

Hald, M., Sættern, J. and Nesse, E. (1990) Middle and Late Weichselian stratigraphy in shallow drillings from the southwestern Barents Sea: foraminiferal, amino acid and radiocarbon evidence. *Norsk Geologisk Tidsskrift* **70**, 241–257.

Hebbeln, D., Dokken, T., Andersen, E.S., Hald, M. and Elverhøi, A. (1994) Moisture supply for northern ice-sheet growth during the last glacial maximum. *Nature* **370**, 357–360.

Horn, G. and Orvin, A.K. (1928) Geology of Bear Island. *Norsk Polarinstitutt Skrifter* **15**, 1–162.

Hughes, T.J. (1979) Reconstruction and disintegration of ice sheets for the CLIMAP 18 000 and 125 000 years experiments: theory. *Journal of Glaciology* **24**, 493–495.

Hughes, T.J. (1981) Numerical reconstructions of ice sheets. *In*: Denton, G.H. and Hughes, T.J. (eds), *The Last Great Ice Sheets*, pp. 221–261. John Wiley & Sons, New York.

Hughes, T.J. (1987) The marine transgression hypothesis. *Geografiska Annaler* **69**, 237–250.

Isaksson, E. (1992) The western Barents Sea and the Svalbard archipelago 18 000 years ago a finite-difference computer model reconstruction. *Journal of Glaciology* **38**, 295–301.

Jones, G.A. and Keigwin, L.D. (1988) Evidence from Fram Strait (78° N) for early deglaciation. *Nature* **336**, 56–59.

Karlén, W. (1987) Geomorfologi, glaciologi och istidsförlopp på östra Svalbard. *In*: Hoppe, G., Björn-Rasmussen, S. and Roland, M.W. (eds), *Expeditionen Ymer-80-en slutrapport*, pp. 88–92. Kungliga Vetenskapsakademien, Stockholm.

Koç, N., Jansen, E. and Haflidason, H. (1993) Paleoceanographic reconstructions of surface ocean conditions in the Greenland, Iceland and Norwegian Seas through the last 14-ka based on diatoms. *Quaternary Science Reviews* **12**, 115–140.

Laberg, J.S. and Vorren, T.O. (1995) Late Weichselian submarine debris flow deposits on the Bear Island trough mouth fan. *Marine Geology* **127**, 45–72.

Laberg, J.S. and Vorren, T.O. (1996) The Middle and Late Pleistocene evolution of the Bear Island trough mouth fan. *Global and Planetary Change* **12**, 309–330.

Lambeck, K. (1993) Glacial rebound and sea-level change: an example of a relationship between mantle and surface processes. *Tectonophysics* **223**, 15–37.

Lambeck, K. (1995) Constraints on the Late Weichselian ice sheet over the Barents Sea from observations of raised shorelines. *Quaternary Science Reviews* **14**, 1–16.

Lambeck, K. (1996) Limits on the areal extent of the Barents Sea ice sheet in Late Weichselian time. *Global and Planetary Change* **12**, 41–51.

Landvik, J.Y. and Salvigsen, O. (1985) Glaciation development and interstadial sea-level on central Spitsbergen Svalbard. *Polar Research* **3**, 1–10.

Landvik, J.Y., Mangerud, J. and Salvigsen, O. (1987) The Late Weichselian and Holocene shoreline displacement on the west-central coast of Svalbard. *Polar Research* **5**, 2944.

Landvik, J.Y., Bolstad, M., Lycke, A.K., Mangerud, J. and Sejrup, H.P. (1992a) Weichselian stratigraphy and palaeoenvironments at Bellsund, western Svalbard. *Boreas* **21**, 335–358.

Landvik, J.Y., Hansen, A., Kelly, M., Salvigsen, O., Slettemark, Ø. and Stubdrup, O.P. (1992b) The last deglaciation and glacimarine/marine sedimentation on Barentsøya and Edgeoya, eastern Svalbard. *Lundqua Report* **35**, 61–83.

Landvik, J.Y., Hjort, C., Mangerud, J., Möller, P. and Salvigsen, O. (1995) The Quaternary record of eastern Svalbard—an overview. *Polar Research* **14**, 95–103.

Lavrushin, J.A. (1967) *Plejstocen zapadnogo Spicbergena* (Pleistocene of Vestspitsbergen) Doklady Akademii Nauk SSSR, Vol. 176, pp. 167–170. (Internal English translation, Norwegian Polar Research Institute, Oslo).

Lavrushin, J.A. (1969) *Cetverticnye otlozenija Spicbergena* (Quaternary deposits of Spitsbergen) Pour VIII Congres de l'INQUA, Paris 1969. Nauka, Moskva, pp. 1–177. (Internal English translation, Norwegian Polar Research Institute, Oslo)

Lehman, S.J. and Forman, S.L. (1987) Glacier extent and sea level variation during the Late Weichselian on northwest Spitsbergen Svalbard. *Polar Research* **5**, 271–272.

Lehman, S.J. and Forman, S.L. (1992) Late Weichselian glacier retreat in Kongsfjorden, west Spitsbergen Svalbard. *Quaternary Research* **37**, 139–154.

Liestøl, O. (1972) Submarine moraines off the west coast of Spitsbergen. *Norsk Polarinstitutt Årbok* 1970, pp. 165–168. Norsk Polarinstitutt, Oslo.

Lindner, L. and Marks, L. (1993) Middle and Late Pleistocene evolution of the Hornsund region, south Spitsbergen. *Polish Polar Research* **14**, 275–292.

Lindstrom, D.R. (1990) The Eurasian ice sheet formation and collapse resulting from natural atmospheric CO_2 concentration variations. *Paleoceanography* **5**, 207–227.

Lubinski, D.J., Korsun, S., Polyak, L., Forman, S.L., Lehman, S.J., Herlihy, F.A. and Miller, G.H. (1996) The last deglaciation of the Franz Victoria Trough, northern Barents Sea. *Boreas* **25**, 89–100.

Mahaffy, M.W. (1976) A three-dimensional numerical model of ice sheets: teats on the Barnes ice cap, Northwest Territories. *Journal of Geophysical Research* **81**, 1059–1066.

Manabe, S. and Bryan, K. Jr. (1985) CO_2-induced change in a coupled ocean-atmosphere model, and its paleoclimatic implications. *Journal of Geophysical Research* **90**, 11689–11707.

Mangerud, J. (1977) Late Weichselian marine sediments containing shells, foraminifera, and pollen at Ågotnes, western Norway. *Norsk Geologisk Tidsskrift* **57**, 23–54.

Mangerud, J. and Gulliksen, S. (1975) Apparent radiocarbon ages of recent marine shells from Norway, Spitsbergen, and Arctic Canada. *Quaternary Research* **5**, 263–273.

Mangerud, J. and Salvigsen, O. (1984) The Kapp Ekholm section Billefjorden, Spitsbergen: a discussion. *Boreas* **13**, 155–158.

Mangerud, L., Bolstad, M., Elgersma, A., Helliksen, D., Landvik, J. Y., Lycke, A.K., Lønne, I., Salvigsen, O., Sandahl, T. and Sejrup, H.P. (1987) The Late Weichselian glacial maximum in western Svalbard. *Polar Research* **5**, 275–278.

Mangerud, J. and Svendsen, J.I. (1990) Deglaciation chronology inferred from marine sediments in a proglacial lake basin, western Spitsbergen, Svalbard. *Boreas* **19**, 249–272.

Mangerud, L., Bolstad, M., Elgersma, A., Helliksen, D., Landvik, J.Y., Lønne, L., Lycke, A.K., Salvigsen, O., Sandahl, T. and Svendsen, J.I. (1992) The last glacial maximum on Spitsbergen Svalbard. *Quaternary Research* **38**, 1–31.

Mangerud, J. and Svendsen, J.I. (1992) The last interglacial–glacial period on Spitsbergen Svalbard. *Quaternary Science Reviews* **11**, 633–664.

Mangerud, J., Astakhov, V., Svendsen, J.I. and Tveranger, J. (1993a) PECHORA: Paleo Environment and Climate History of the Russian Arctic. *Nordiska Geologiska Vintermötet. Abstracts*, Tekniska Högskolan i Luleå, Luleå. 132.

Mangerud, J., Astakhov, V., Svendsen, J.I. and Tveranger, J. (1993b) The Barents Ice Sheet margin in Arctic Russia: Preliminary results. *European Science Foundation. PONAM Fourth Annual Workshop*, Scott Polar Research Institute, Cambridge.

Mangerud, J., Dokken, T.M., Hebbeln, D., Heggen, B., Ingólfsson, O., Landvik, J.Y., Mejdahl, V., Svendsen, J.I. and Vorren, T.O. (1998) Fluctuations of the Svalbard–Barents Sea ice sheet the last 150 000 years. *Quaternary Science Reviews* **17**, 11–42.

Marthinussen, M. (1974) Contributions to the Quaternary geology of north-eastmost Norway and the closely adjoining foreign areas. *Norges geologiske undersøkelse* **315**, 1–157.

Matishov, G.G. (1980) Geomorphological signs of the action of the Scandinavian, Novaya Zemlya, and Spitsbergen ice sheets on the floor of the Barents Sea. *Oceanology* **30**, 440–447.

Miller, G.H. (1982) Quaternary depositional episodes, western Spitsbergen, Norway: aminostratigraphy and glacial history. *Arctic and Alpine Research* **14**, 321–340.

Miller, G.H. and Brigham-Grette, J. (1989) Amino acid geochronology: resolution and precision in carbonate fossils. *Quaternary International* **1**, 111–128.

Miller, G.H., Sejrup, H.P., Lehman, S.J. and Forman, S.L. (1989) Glacial history and marine environmental change during the last interglacial–glacial cycle, western Spitsbergen Svalbard., *Boreas* **18**, 273–296.

Møller, J.J. (1987) Shoreline relation and prehistoric settlement in northern Norway. *Norsk geografisk Tidsskrift* **41**, 45–60.

Nathorst, A.G. (1899) Några upplysningar till den nya kartan över Beeren Eiland. *Ymer* **19**, 171–185.

Näslund, J.-O., Zale, R. and Glazovskiy, A. (1994) The mid Holocene transgression on Alexandra Land Franz Josef Land, Russia. *Geografiska Annaler* **76A**, 97–101.

Oerlemans, J. and van der Veen, C.J. (1984) *Ice Sheets and Climate*, Reidel Publishing Company.

Olsson, I.U., El-Gammal, S. and Göksu, Y. (1969) Uppsala natural radiocarbon measurements—IX. *Radiocarbon* **11**, 515–544.

Österholm, H. (1990) The Late Weichselian glaciation and Holocene shore displacement on Prins Oscars Land Nordaustlandet, Svalbard. *Geografiska Annaler* **72A**, 301–317.

Paterson, W.S.B. (1994) *The Physics of Glaciers*. Pergamon Press, Oxford.

Payne, A.J., Sugden, D.E. and Clapperton, C.M. (1989) Modelling the growth and decay of the Antarcic peninsula ice sheet. *Quaternary Research* **31**, 119–134.

Peltier, W.R. (1988) Global sea level and Earth rotation. *Science* **240**, 895–901.

Pelto, M.S., Higgins, S.M., Hughes, T.J. and Fastook, J.L. (1990) Modelling mass-balance changes during a glaciation cycle. *Annals of Glaciology* **14**, 238–241.

Pelto, M.S. and Warren, C.R. (1991) Relationship between tidewater glacier calving velocity and water depth at the calving front. *Annals of Glaciology* **15**, 115–118.

Polyak, L. and Solheim, A. (1994) Late and postglacial environments in the northern Barents Sea west of Franz Josef Land. *Polar Research* **13**, 197–207.

Polyak, L., Lehman, S.J., Gataullin, V. and Jull, A.J.T. (1995) Two-step deglaciation of the southern Barents Sea. *Geology* **23**, 567–571.

Punkari, M. (1995) Glacial flow systems in the zone of confluence between the Scandinavian and Novaya Zemlya ice sheets. *Quaternary Science Reviews* **14**, 589–603.

Robin, G. de Q. (1955) Ice movement and temperature distribution in glaciers and ice sheets. *Journal of Glaciology* **3**, 589–606.

Rutter, N. (1995) Problematic ice sheets. *Quaternary International* **28**, 19–37.

Salvigsen, O. (1977) Radiocarbon datings and the extension of the Weichselian ice-sheet in Svalbard. *Norsk Polarinstitutt Årbok* 1976, pp. 209–224. Norsk Polarinstitutt, Oslo.

Salvigsen, O. (1978) Holocene emergence and finds of pumice, whalebones, and driftwood at Svartknausflya, Nordaustlandet. *Norsk Polarinstitutt Årbok* 1977, pp. 217–228. Norsk Polarinstitutt, Oslo.

Salvigsen, O. (1979) The last deglaciation of Svalbard. *Boreas* **8**, 229–231.

Salvigsen, O. (1981) Radiocarbon dated raised beaches in Kong Karls Land, Svalbard, and their consequences for the glacial history of the Barents Sea. *Geografiska Annaler* **63A**, 280–291.

Salvigsen, O. and Nydal, R. (1981) The Weichselian glaciation in Svalbard before 15 000 B.P. *Boreas* **10**, 433–446.

Salvigsen, O. and Österholm, H. (1982) Radiocarbon dated raised beaches and glacial history of the northern coast of Spitsbergen Svalbard. *Polar Research* **1**, 97–115.

Salvigsen, O., Elgersma, A., Hjort, C., Lagerlund, E., Liestøl, O. and Svensson, N.-O. (1990) Glacial history and shoreline displacement on Erdmannflya and Bohemanflya Spitsbergen, Svalbard. *Polar Research* **8**, 261–273.

Salvigsen, O. and Mangerud, J. (1991) Holocene shoreline displacement at Agardhbukta Spitsbergen, Svalbard. *Polar Research* **9**, 1–7.

Salvigsen, O. and Elgersma, A. (1993) Radiocarbon dating of deglaciation and raised beaches in northwestern Sorkapp Land Spitsbergen, Svalbard. *Prace Geograficzne* **94**, 39–48.

Salvigsen, O., Adrielsson, L., Hjort, C., Kelly, M., Landvik, J.Y. and Ronnert, L. (1995) Dynamics of the last glaciation in eastern Svalbard as inferred from glacier-movement indicators. *Polar Research* **14**, 141–152.

Salvigsen, O. and Slettemark, Ø. (1995) Past glaciations and sea levels on Bjørnøya Svalbard. *Polar Research* **14**, 245–251.

Schytt, V., Hoppe, G., Blake, W., Jr. and Grosswald, M.G. (1968) A preliminary report about the Stockholm University Svalbard Expedition 1966. The extent of the Würm glaciation in the European Arctic, pp. 207–216.

Siegert, M.J. and Dowdeswell, J.A. (1995a) Numerical modelling of the Late Weichselian Svalbard–Barents Sea ice sheet. *Quaternary Research* **43**, 1–13.

Siegert, M.J. and Dowdeswell, L.A. (1995b) Modelling ice-sheet sensitivity to late Weichselian environments in the Svalbard–Barents Sea region. *Journal of Quaternary Science* **10**, 33–43.

Siegert, M.J. and Fjeldskaar, W. (1996) Isostatic uplift in the Late Weichselian Barents Sea: implications for ice-sheet growth. *Annals of Glaciology* **23**, 352–358.

Snyder, J.A., Korsun, S.A. and Forman, S.L. (1996) Postglacial emergence and the tapes transgression, north-central Kola Peninsula Russia. *Boreas* **25**, 47–56.

Solheim, A. and Kristoffersen, Y. (1984) The physical environment Western Barents Sea, 1: 1,500,000. Sediments above the upper regional unconformity: thickness, seismic stratigraphy and outline of the glacial history. *Norsk Polarinstitutt Skrifter* **179B**, 1–26.

Solheim, A., Russwurm, L., Elverhøi, A. and Berg, M.N. (1990) Glacial geomorphic features in the northern Barents Sea: direct evidence for grounded glacier icelacial geomorphic features in the northern Barents Sea: direct evidence for grounded glacier ice and implications for the pattern of deglaciation and late glacial sedimentation. In: Dowdeswell, J.A. and Scourse, J.D. (eds), *Glacimarine environments: Processes and sediments, Geological Society Special Publication*, **53**, 253–268.

Solheim, A., Andersen, E.S., Elverhøi, A. and Fiedler, A. (1996) Late Cenozoic depositional history of the western Svalbard continental shelf, controlled by subsidence and climate. *Global and Planetary Change* **12**, 135–148.

Sollid, J.L., Andersen, S., Hamre, N., Kjeldsen, O., Salvigsen, O., Sturød, S., Tveitå, T. and Wilhelmsen, A. (1973) Deglaciation of Finnmark, North Norway. *Norsk geografisk Tidsskrifot* **27**, 233–325.

Stuiver, M. and Reimer, P. (1993) Extended ^{14}C data base and revised Calib 3.0 ^{14}C age calibration program. *Radiocarbon* **35**, 215–230.

Svendsen, J.I., Mangerud, J. and Miller, G.H. (1989) Denudation rates in the Arctic estimated from lake sediments on Spitsbergen Svalbard. *Palaeogeography, Palaeoclimatology, Palaeoecology* **76**, 153–168.

Svendsen, J.I. and Mangerud, J. (1992) Paleoclimatic inferences from glacial fluctuations on Svalbard during the last 20 000 years. *Climate Dynamics* **6**, 213–220.

Svendsen, J.I., Mangerud, J., Elverhøi, A., Solheim, A. and Schüttenhelm, R.T.E. (1992) The Late Weichselian glacial maximum on western Spitsbergen inferred from offshore sediment cores. *Marine Geology* **104**, 1–17.

Svendsen, J.J., Elverhøi, A. and Mangerud, J. (1996) The retreat of the Barrents ice sheet on the western Svalbard margin. *Boreas* **25**, 244–256.

Svendsen, J.I. and Mangerud, J. (1997) Holocene glacial and climatic variations on Spitsbergen Svalbard. *The Holocene* **7**, 45–57.

Sættem, J. (1990) Glaciotectonic forms and structures on the Norwegian continental shelf: observations, processes and implications. *Norsk Geologgisk Tidsskrift* **70**, 81–94.

Sørensen, R., Bakkelid, S. and Torp, B. (1987) Nasjonalatlas for Norge. Kartblad 2.3.3. Scale 1:5000 000. *Land Uplift*. Statens Kartverk, Hønefoss.

Troitsky, L., Punning, J.-M., Hütt, G. and Rajamae, R. (1979) Pleistocene glaciation chronology of Spitsbergen. *Boreas* **8**, 401–407.

Tushingham, A.M. and Peltier, W.R. (1991) A new global model of Late Pleistocene deglaciation based upon geophysical predictions of post glacial relative sea level change. *Journal of Geophysical Research* **96**, 4497–4523.

Tushingham, A.M. and Peltier, W.R. (1993) Implications of the radiocarbon timescale for ice sheet chronology and sea-level change. *Quaternary Research* **39**, 125–129.

Tveranger, J., Astakhov, V., Mangerud, J. (1995) The margin of the last Barents–Kara ice sheet at Markhida, northern Russia. *Quaternary Research* **44**, 328–340.

Vorren, T.O. and Kristoffersen, Y. (1986) Late Quaternary glaciation in the southwestern Barents Sea. *Boreas* **15**, 51–60.

Vorren, T.O., Vorren, K.D., Alm, T., Gulliksen, S. and Løvlie, R. (1988) The last deglaciation (20 000 to 11 000 B.P.) on Andøya, northern Norway. *Boreas* **17-77**, 41–77.

Vorren, T.O., Lebesbye, E., Andreassen, K. and Larsen, K.-B. (1989) Glacigenic sediments on a passive continental margin as exemplified by the Barrents Sea. *Marine Geology* **85**, 251–272.

Vorren, T.O., Lebesbye, E. and Larsen, K.B. (1990) Geometry and genesis of the glacigenic sediments in the southern Barents Sea. In: Dowdeswell, J.A. and Scourse, J.D. (eds), *Glacimarine Environments: Processes and Sediments. Geological Society Special Publication*, **53**, 269–288.

Vorren, T.O., Rokoengen, K., Bugge, T. and Larsen, O.A. (1992) *Kontinentalsokkelen. Tykkelsen på kvartære sedimenter*, 1:3 *mill*. Nasjonalatlas for Norge. Statens Kartverk, Honefoss.

Vorren, T.O. and Laberg, J.S. (1996) Late glacial air temperature, oceanographic and ice sheet interactions in the southern Barents Sea region. In *Late Quaternary Palaeoceanography of the North Atlantic margins. Geological Society Special Publication*, eds J.T. Andrews, W.E.N. Austin, H. Bergsten, and A.E. Jennings, Vol. 111, pp. 303–321.

Vorren, T.O., Laberg, J.S., Blaume, F., Dowdeswell, J.A., Kenyon, N.H., Mienert, J., Rumohr, J. and Werner, F. (1998) The Norwegian–Greenland continental margins: morphology and late Quaternary sedimentary processes and environment. *Quaternary Science Reviews* **17**, 273–302.

Wohlfarth, B., Lemdahl, G., Olsson, S., Persson, T., Snowball, I., Ising, J. and Jones, V. (1995) Early Holocene environment on Bjørnøya (Svalbard) inferred from multidisciplinary lake sediment studies. *Polar Research* **14**, 253–275.